Modelling the fluid phase behaviour of aqueous mixtures of multifunctional alkanolamines and carbon dioxide using transferable parameters with the SAFT-VR approach

J. Rodriguez, N. Mac Dowell, F. Llovell, C. S. Adjiman, G. Jackson and A. Galindo*
Department of Chemical Engineering, Imperial College London,
and Centre for Process Systems Engineering,
South Kensington Campus, London SW7 2AZ
**Corresponding author: a.galindo@imperial.ac.uk*

PACS numbers:

Abstract

Among the many applications that alkanolamines find in industry, carbon dioxide (CO_2) capture from large stationary sources is becoming most relevant. Aqueous mixtures of amines and CO_2 have a complex behaviour, characterised by extensive hydrogen bonding and other types of chemical reactions. An implicit treatment of the key reactions via appropriate association schemes has been shown to provide a promising physical basis for the modelling of these systems. Here, we introduce association models for use with SAFT-VR for some of the more promising multifunctional alkanolamines in the context of CO_2 capture: monoethanolamine (MEA), 2-amino-2-methyl-1-propanol (AMP), diethanolamine (DEA) and methyldiethanolamine (MDEA), and their mixtures with H_2O and CO_2. A revised model of the MEA + H_2O + CO_2 mixture is also presented with an extension to high temperature. Excellent predictive capabilities are demonstrated for pure components and binary aqueous mixtures. Good overall results are also obtained for the ternary aqueous mixtures of alkanolamines and CO_2, particulary for DEA and MDEA. Furthermore, the degree of speciation is successfully predicted for the MEA + H_2O + CO_2 mixture. Since only a limited number of parameters need to be estimated from vapour-liquid equilibrium data, the ternary SAFT-VR reaction-implicit models developed in this work offer a useful initial assessment of the different solvents and blends.

I. INTRODUCTION

Multifunctional alkanolamines, molecules containing both amine and hydroxyl functional groups, are common in natural products. For example amino acids such as hydroxyproline as well as hormones and neurotransmitters such as epinephrine (adrenaline) and norepinephrine (noradrenaline) are alkanolamines[1]. Furthermore, alkanolamines are versatile compounds that find application across a range of industries: they are used as beta blockers (propranolol) as well as surfactants, corrosion inhibitors and for pH adjustment. Another area where alkanolamines have traditionally found significant application is in the removal of acid gases such as hydrogen sulfide (H_2S) from gas streams in oil and gas refineries[2].

More recently, in light of growing concern surrounding anthropogenic carbon dioxide (CO_2) emissions[3], there has been a great deal of renewed interest in alkanolamine-based chemisorption processes as part of the effort to mitigate these emissions, particularly from large fixed-point emission sources such as fossil-fuel fired power-stations[4,5]. Solvents that are receiving particular attention include monoethanolamine (MEA), diethanolamine (DEA), methyldiethanolamine (MDEA) and 2-amino-2-methyl-1-propanol (AMP)[5]. The large-scale deployment of alkanolamine-based CO_2 capture technology will entail a significant economic penalty[6], and the reduction of this cost is a well recognised imperative[7]. As it is the thermophysical properties of these alkanolamine solvents in aqueous mixtures with CO_2 that define the limits of process operation, the availability of accurate and predictive models of these fluids is vital in the optimal design and operation of CO_2 capture processes.

In this paper, we describe the use of the statistical associating fluid theory for potentials of variable range (SAFT-VR)[8–12] to calculate the equilibrium fluid-phase behaviour of aqueous mixtures of multifunctional alkanolamines and CO_2. The first successful description of associating and reacting systems is the chemical theory of solutions developed by Dolezalek[13–15]. In this type of chemical approach one postulates the existence of distinct molecular species in solution, which are assumed to be in chemical equilibrium. For associating systems the strong anisotropic hydrogen-bonding (physical) interactions are treated as chemical reactions with corresponding equilibrium constants. An important disadvantage with a chemical treatment lies in having to account for all of the equilibrium species and corresponding reaction mechanisms. After assuming a particular equilibrium scheme, one is then faced with the problem of determining the equilibrium constants together with their temperature and concentration/density dependences. This limits the predictive capabilities of chemical theories, though with appropriate experimental data the approach can be used very successfully to represent the behaviour of highly non-ideal solutions when other approaches are inappropriate. From a seemingly diametric physical standpoint, originally attributed to van Laar[16,17] and his followers, the existence of any molecular species other than the unreacted components is denied, and the properties of the mixture are attributed to large differences in the intermolecular interactions between the species which may lead to aggregation. While the opposing chemical and physical perspectives to dealing with reactive mixtures led to "harsh polemic" from the very beginning[18], it is now recognized that the Dolezalek and van Laar views are but extreme representations of the actual situation: the distinction between chemical and physical forces is often arbitrary and in many cases the designation of a mixture as "chemical" or "physical" is only a matter of taste or convenience[19]. It is reasonable to assume that a physical treatment is appropriate when the "reactions" do not lead to species which are very different chemically, particularly in the case of reversible reactions, but of course this will not be the case when the products are significantly distinct from the reactants. Equations of state of the SAFT family are cast as physical theories of the liquid state. In developing our SAFT-VR models of carbon dioxide in aqueous alkanolamine solvents we implicitly assume a physical model of the reversible chemical reactions involved in the absorption process: a strong association interaction is used to mimic the aggregation processes in solution whereby after complete "reaction" each carbon dioxide molecule is associated to one or two molecules of the alkanolamine, depending on the stoichiometry of the reaction. Economou and Donohue[20] have shown that a SAFT treatment is equivalent to the chemical or quasi-chemical approaches as long as the correct reaction stoichiometry is incorporated. It is also important to point out that the reactions involved in the mixtures of CO_2 in aqueous alkanolamines involve the formation of charged species. Though the SAFT-VR approach has been extended to describe electrolyte solutions[21,22] we do not consider ionic speciation explicitly in our current work. The reactions are instead assumed to involve the association of the various species as aggregates (bound ion pairs) with no net overall charge. The dielectric constant of the alkanolamine solutions are 2 to 5 times lower that of pure water, which would certainly be consistent with conditions where one would expect ion pairing, particularly at higher temperatures.

In a previous paper[23] it was shown that, in order to model accurately aqueous mixtures of MEA and CO_2 with an approach based on the statistical associating fluid theory SAFT-VR, it is vital to distinguish between the amine and hydroxyl functional groups in developing an association scheme. The main drawback of incorporating such a level of molecular detail is the introduction of extra molecular parameters required to characterise these molecules, as compared to a simpler treatment of molecular interactions. This places an additional burden on parameter estimation, and requires additional data to derive statistically significant parameter values. To circumvent this issue, we reduce the number of parameters to be estimated by transferring some SAFT-VR molecular interaction from models of monofunctional compounds to models of multifunctional compounds. We also apply this approach to mixtures, transferring the molecular parameters describing the unlike association interactions from mixtures of monofunctional associating compounds to mixtures of multifunctional associating compounds. This approach to model development preserves a high level of molecular detail whilst minimising the number of intermolecular model parameters that need to be determined. Furthermore, the methodology facilitates the development of detailed molecular models in the absence of extensive experimental data.

There have been extensive previous investigations of the thermophysical properties and fluid-phase behaviour of alkanolamines, and a complete review of the literature covering this area is beyond the scope of our paper. Thus, only work which also utilises a Wertheim-like description of association interactions and some of the more recent contributions using popular methods are discussed here. One approach which has often been used to describe the fluid-phase behaviour of the alkanolamines is the eNRTL theory[24,25]. It is worth noting that whilst the original version of the eNRTL approach has been applied to alkanolamine systems by several authors[26–28], it has recently been shown by Bollas et al.[29] that the original eNRTL leads to an inconsistent description of mixtures containing multiple anions and/or cations. To this end, Bollas et al.[29] presented an improved version, specifically for application to multi-electrolyte systems. This approach was then successfully used by Hessen et al.[30] to describe the fluid-phase behaviour of aqueous mixtures of alkanolamines and CO_2. A different version of the eNRTL model[31] has been employed by Zhang and Chen[32] to calculate the thermodyanmic properties of the MDEA + H_2O + CO_2 system. Another relevant approach is the extended UNIQUAC treatment of Thomsen et al.[33,34], which has been used recently by Faramarzi et al.[35,36] to study the absorption of CO_2 in aqueous solutions of alkanolamines.

Equation of state approaches have also been used to describe the fluid-phase behaviour of alkanolamine systems. The electrolyte equation of state presented by Fürst and Renon[37] has been used in several contributions[38–40] to describe the fluid-phase behaviour of the absorption of CO_2 in aqueous alkanolamine mixtures. Huang and Radosz[41] have presented models for a number of primary, secondary and tertiary amines, including diethylamine. They modelled diethylamine as a self-associating compound, and used a two-site association scheme to do this. Button and Gubbins[42] used the original SAFT approach[41,43] to model the vapour-liquid equilibria of mixtures of CO_2 + MEA + H_2O and CO_2 + DEA + H_2O. They explicitly recognised the multifunctional nature between the molecules, but did not include the asymmetry of the association of the alkanolamines in their model. Despite the simplified description of the hydrogen-bonding interactions in the model, Button and Gubbins presented an accurate description of the vapour-liquid equilibrium of both the pure alkanolamines and the aqueous solutions using a single temperature-independent unlike binary parameter. They also presented predictions for the ternary mixtures of alkanolamines, water and carbon dioxide, but the deviations of the model from the experimental data are significant. These results are consistent with the conclusions presented in a previous work[23], where the benefit of explicitly describing the individual functional groups did not become apparent until multicomponent mixtures were studied. Avlund et al.[44] have applied the cubic plus association (CPA) equation of state[45] to aqueous mixtures of alkanolamines using a 4-site association scheme for all the compounds. While the multifunctional nature of the alkanolamines was recognised, they do not discriminate between the properties of the different functional groups. Despite this simplification, their models accurately describe the fluid-phase behaviour of aqueous mixtures of MEA, DEA and MDEA. This work has been recently improved and compared with the sPC-SAFT equation of state[46]. However, no attempt is made to model ternary mixtures including CO_2. Sánchez et al.[47,48] have recently applied the group contribution with association equation of state (GCA-EOS)[49] to predict the phase behaviour of MEA, DEA, MDEA and their aqueous mixtures, with very promising results. Finally, Rozmus et al[50] have succesfully applied a group contribution method based on the PC-SAFT equation of state (GC-PPC-SAFT)to describe the phase behaviour of amines and their mixtures with alkanes and alcohols.

In our current work, we use the statistical associating fluid theory for potentials of variable range (SAFT-VR)[8,9]. The theory and methodology used to determine appropriate values for the molecular parameters have been presented in detail in our previous papers[23,51], so that only a brief overview is presented in Section II. We explicitly distinguish between the interactions between the different functional groups and present new, transferable models of sterically hindered (AMP), secondary (DEA), and tertiary (MDEA) alkanolamine compounds, as pure fluids, in aqueous mixtures, and in aqueous mixtures with CO_2. For completeness, and to correct a number of typographical errors in reference

[23], we also present revised model parameters for MEA and its mixtures with H_2O and CO_2. We should note here that the ternary mixtures of alkanolamines, H_2O and CO_2 are reactive – i.e., new species are formed (see references[52–55] for detailed studies on the class of reactions involved in these mixtures). The main contribution of our approach resides in the ability of our ternary association models to describe the fluid phase behaviour of the mixtures of alkanolamines, H_2O and CO_2 without explicitly accounting for the complex reaction mechanisms characteristic of these mixtures. However, speciation calculations can be carried out within the SAFT-VR framework; this capability is illustrated using the MEA + CO_2 + H_2O system. The implicit treatment of the reactions provides a promising method for early assessment of new compounds, since solvent models that offer a reasonably good performance can be obtained by estimating a small number of parameters from vapour-liquid equilbrium data alone. The pure component models are introduced in Section III, the aqueous mixtures models in Section IV, and the ternary mixture models in Section V.

II. THEORY, MODELS AND METHODOLOGY

A. Molecular models

Following the SAFT-VR approach, a molecule i is modelled as a single square-well segment in the case of H_2O or a homonuclear chain of m_i bonded square-well segments of hard-core diameter σ_{ii} when non-spherical molecules are considered (Figure 1). The square-well interactions are further characterised by an attractive well depth ε_{ii} and a range λ_{ii}. Though the SAFT-VR formalism employed involves fluids of molecules formed from square-well segments, the approach is generic and can be used for other forms of the segment-segment interactions such as the Lennard-Jones[56], Yukawa[57] and Mie[58,59] potentials.

A number of off-centre, square-well bonding sites are used to mediate strong, anisotropic association interactions. In order to fully specify the molecular model, the number of site types and the number of sites of each type must be specified. The sites are placed at a reduced distance $r_d^* = r_d/\sigma_{ii} = 0.25$ from the centre of a segment. The cut-off range between a site a on a molecule i and a site b on a molecule j is denoted by $r_{c;ab,ij}^* = r_{c;ab,ij}/\sigma_{ij}$. These parameters define the volume $K_{ab,ij}$ available for site-site bonding[60]. When two sites come within a distance $r_{c;ab,ij}^*$, they interact via a square-well potential with a well depth $\varepsilon_{ab,ij}^{HB}$.

The sites are often labelled as e or H, representing either an electronegative atom (or lone electron pairs) or a hydrogen atom in a molecule, respectively; in such cases only e-H bonding is allowed.

In order to model mixtures, a number of unlike intermolecular potential parameters also need to be specified. The arithmetic mean (sometimes referred to as the Lorentz rule[61]) is used to obtain size-related unlike intermolecular parameters such as the unlike segment size $\sigma_{ij} = (\sigma_{ii} + \sigma_{jj})/2$ and the range of the unlike dispersion interaction $\lambda_{ij} = (\sigma_{ii}\lambda_{ii} + \sigma_{jj}\lambda_{jj})/(\sigma_{ii} + \sigma_{jj})$. These parameters are typically not readjusted at any point. The unlike dispersion energy between two components i and j is characterised by a strength ε_{ij}, and the unlike hydrogen bonding energy between a site a on molecule i and a site b on molecule j is similarly characterised by a strength $\varepsilon^{HB}_{ab,ij}$ and and range $r^{*}_{c;ab,ij}$. Although combining rules for the energetic parameters can be proposed[9,62], they are not usually predictive for hydrogen-bonding interactions. Instead, these are treated as adjustable parameters and ε_{ij} and $\varepsilon^{HB}_{ab,ij}$ (and $r^{*}_{c;ab,ij}$ where necessary) are determined by parameter estimation using experimental fluid-phase equilibrium data.

B. The SAFT-VR Equation of State

The Helmholtz free energy A of a mixture of associating chain molecules can be written in the usual SAFT form as[8,43,63,64]

$$\frac{A}{NkT} = \frac{A^{IDEAL}}{NkT} + \frac{A^{MONO.}}{NkT} + \frac{A^{CHAIN}}{NkT} + \frac{A^{ASSOC.}}{NkT}, \tag{1}$$

where N is the number of molecules, k the Boltzmann constant, and T the absolute temperature. The term A^{IDEAL} corresponds to the ideal free energy of the mixture, and $A^{MONO.}$, A^{CHAIN}, and $A^{ASSOC.}$ are residual contributions to the free energy due to the repulsive and attractive (dispersion) interactions between monomeric segments, to the formation of chains, and to site-site intermolecular association, respectively. For further details of the SAFT-VR approach and of the specific expressions used, the reader is referred to the original papers[8,9]. The pressure and chemical potential, required for the solution of phase equilibrium, are obtained directly using standard thermodynamic relations:

$$P = -\left.\frac{\delta A}{\delta V}\right|_{T,V} \quad \text{and} \quad \mu_i = -\left.\frac{\delta A}{\delta N_i}\right|_{T,V} . \tag{2}$$

The interfacial tension is calculated using a density functional theory formulated (DFT) within SAFT-VR. In an inhomogeneous system, the total Helmholtz energy of the system becomes a functional, as the number density depends on the position of a particle, so $A[\{\rho_m(\mathbf{r})\}]$ with $m = 1$ to n, the total number of components). The minimum value of grand potential functional, $\Omega[\{\rho_m(\mathbf{r})\}]$, is the equilibrium grand potential of the system which must satisfy the condition[65]

$$\left.\frac{\delta\Omega[\{\rho_m(\mathbf{r})\}]}{\delta\rho_i(\mathbf{r})}\right|_{\mathrm{eq}} = \left.\frac{\delta A[\{\rho_m(\mathbf{r})\}]}{\delta\rho_i(\mathbf{r})}\right|_{\mathrm{eq}} - \mu_i = 0, \tag{3}$$

where μ_i is the chemical potential of component i. Hence, the minimisation of the grand potential function expressed in equation (3) has two terms: a reference contribution, that corresponds to the local chemical potential μ^{ref} and can be obtained from the expressions for the homogeneous system at the local density, and an attractive contribution, that is obtained with a perturbative scheme using an average value of the correlation function for the bulk fluid. The equilibrium density profiles for each component are found by solving the corresponding Euler-Lagrange relations. Calculations are done in one dimension for a free planar interface. The details of the numerical aspects of this procedure are described in a previous publications[66–68]. Once the equilibrium density profile is known, the surface tension is determined by using the thermodynamic relation $\gamma = (\Omega + PV)/\mathcal{A}$, where $\mathcal{A}$ is the interfacial area and P is the bulk pressure.

C. Parameter estimation

As is common practice, experimental vapour pressure P_v and saturated liquid density ρ_l data are used in the determination of the pure component intermolecular model parameters. We use of the Chemical Database Service at Daresbury[69] to gain access to Detherm, from where the experimental data employed in this work has been collected. Values for the SAFT-VR molecular parameters are obtained by fixing the chain length m_i (which characterizes the molecular non-sphericity) to a value between 2.0 and 4.0 and carrying out optimisations within this interval taking steps of 0.01 in m_i. At each of these intervals, values for the remaining SAFT-VR parameters were obtained by optimising the theoretical description of the experimental fluid phase equilibrium data from the triple point to 90% of the critical temperature. Critical and near-critical data are avoided in the estimation, as this region cannot be accurately reproduced with analytical equations of state such as SAFT[70]. The Maxwell equal area construction using a steepest-descent method[71] is used to solve for the conditions of phase equilibria in the case of the pure-component phase equilibria. The HELD *(P,T)* flash algorithm[72,73] and the solvers available in the gPROMS software package[74] are used in the case of the phase equilibria for the binary and ternary mixtures. Typically, the parameter estimation problem renders a number of candidate models[75], with equivalent performance in terms of the deviation from experimental data. Hence, we search for a parameter set which is physically meaningful that not only has an acceptable accuracy in representing the vapour liquid equilibria (VLE) data, but that gives a good prediction of the vapour-liquid interfacial tension and/or enthalpy of vaporisation, as well as providing a satisfactory performance in mixture calculations. The performance of the pure models is reported using separate percentage AADs for vapor pressure and liquid density,

$$\mathrm{AAD\%}\ P = \frac{100}{N_P}\sum_{i=1}^{N_P}\left[\frac{P_{v,i}^{exp}(T_i) - P_{v,i}^{calc}(T_i)}{P_{v,i}^{exp}(T_i)}\right]$$

$$\mathrm{AAD\%}\ \rho = \frac{100}{N_\rho}\sum_{j=1}^{N_\rho}\left[\frac{\rho_{l,j}^{exp}(T_j) - \rho_{l,j}^{calc}(T_j)}{\rho_{l,j}^{exp}(T_j)}\right]$$

where N_P is the number of vapour pressure experimental points, N_ρ is the number of saturated liquid density experimental points, $P_{v,i}^{exp}(T_i)$ is the experimental vapour pressure for the i^{th} point, $P_{v,i}^{calc}(T_i)$ is the calculated vapour pressure at the conditions of the i^{th} experimental point, $\rho_{l,j}^{exp}(T_j)$ is the experimental saturated liquid density for the j^{th} point and $\rho_{l,j}^{calc}(T_j)$ is the calculated saturated liquid density at the conditions of the point j^{th}. The adjustable unlike binary interaction parameters ε_{ij}, $\varepsilon_{ab,ij}^{HB}$ and $r_{c,ab,ij}^{*}$ needed to model the binary mixtures of interest are also determined by comparison to mixture VLE data. In the case of mixtures, the error in the calculated equilibrium pressure at a given temperature and liquid composition (AAD% P) and/ or the error in the calculated equilibrium temperature at given pressures and liquid conditions (AAD% T) are reported, as given by the following expressions

$$\mathrm{AAD\%}\ P = \frac{100}{N_P}\sum_{i=1}^{N_P}\left[\frac{P_{i}^{exp}(T_i, x_i^L) - P_{i}^{calc}(T_i, x_i^L)}{P_{i}^{exp}(T_i, x_i^L)}\right],$$

$$\text{AAD\%}\ T = \frac{100}{N_T} \sum_{i=1}^{N_T} \left[\frac{T_i^{exp}(P_i, x_i^L) - P_i^{calc}(P_i, x_i^L)}{P_i^{exp}(P_i, x_i^L)} \right].$$

If available, the error in the composition of the other equilibrium (vapour or liquid) phase at each T_i or P_i and phase I composition is also reported. Since mole fractions are between zero and one, an absolute measure of error is given

$$\text{AAD}\ x^{II} = \frac{1}{N_x} \sum_{i=1}^{N_x} [x_i^{II,exp} - x_i^{II,calc}].$$

Readers are referred to an earlier paper[23] for the exact functional forms of the objective function used to estimate the model parameters in this work.

III. PURE COMPONENTS

Pure H_2O and CO_2 have been investigated in a number of previous studies employing the SAFT-VR equation of state[75–80], and the reader is directed to the the original papers for details. For completeness, the H_2O and CO_2 SAFT-VR model parameters are presented in Table I. In the following subsections, models for the alkanolamines of interest are introduced, as well as parameters for some monofunctional compounds from which association parameters are transferred to the alkanolamine models.

A. Primary alkanolamines: MEA and AMP (transferring association parameters from ethanol and ethylamine)

Among the primary alkanolamines, monoethanolamine (MEA) and 2-amino-2-methyl-1-propanol (AMP) are receiving much attention for carbon capture application. The chemical structures of MEA and AMP are given in Figures 1a) and 1b), respectively. MEA is considered to be the benchmark solvent in the context of carbon capture processes[2]. An extensive study on the development of a SAFT-VR model for pure MEA can be found in a previous paper[23]. Here, the pure MEA model is presented again for the sake of completeness and to correct typographical errors. The AMP molecule is a sterically hindered primary amine that presents a number of theoretical advantages over MEA: AMP reacts with CO_2 to produce a carbamate of relatively low stability which readily hydrolyses to form a bicarbonate, which makes loadings of up to one mole of CO_2 per mole of amine possible[81]; the loaded AMP solvent is also known to require a lower energy of regeneration and to have superior degradation resistance when compared to MEA[81–83].

The intermolecular parameters describing the N-H association between primary amino groups are transferred from a model of ethylamine ($EtNH_2$)[23], see Figure 1c) for the chemical structure and the corresponding SAFT-VR model. The ethylamine interaction parameters[51] are given in Table I and a comparison between experimental VLE data and SAFT-VR description is presented in Figure 2. The SAFT-VR DFT predictions of the vapour-liquid interfacial tension of ethylamine (shown later in Figure 5) are found to be in good agreement with experimental values. In the same fashion, association parameters describing the interaction between the OH groups are transferred from a model of ethanol (EtOH)[23]; (see Figure 1d) for the chemical structure and SAFT-VR model, Table I for the parameter values and Figure 2 for a comparison of the SAFT-VR description with experiments).

In Figure 1a) the chemical structure of the MEA molecule and the model proposed for use with SAFT-VR[23] are presented. MEA is modelled as a chain molecule, where the hydrogen bonding interactions are accounted for via the inclusion of six association sites. Two sites of type e and one site of type H are used to mediate the hydrogen bonding interactions between the hydroxyl groups. One site of type e^* and two sites of type H^* mediate the hydrogen bonding interactions between the amine groups. Sites e and e^* represent the lone pairs of electrons on the oxygen and nitrogen atoms, respectively. Likewise, the H and H^* sites represent the hydrogen atoms on the hydroxyl and amine groups. The parameters describing the OH-OH ($\varepsilon^{HB}_{eH,\mathrm{MEA},\mathrm{MEA}}$ and $r_{c;eH,\mathrm{MEA},\mathrm{MEA}}$) and NH_2-NH_2 ($\varepsilon^{HB}_{e^*H^*,\mathrm{MEA},\mathrm{MEA}}$ and $r_{c;e^*H^*,\mathrm{MEA},\mathrm{MEA}}$) interactions are transferred from ethylamine and ethanol respectively. The cut-off range (which characterises the volume available for bonding) is transferred in its reduced form, i.e., $r^*_{c;eH,\mathrm{MEA},\mathrm{MEA}}$, as defined in Section II, rather than $r_{c;eH,\mathrm{MEA},\mathrm{MEA}}$. Only six other parameters therefore need to be determined for the SAFT-VR model of the MEA fluid[23]. The model parameters are given in Tables II and III. The SAFT-VR description of the vapour-liquid equilibria of MEA are compared against experimental data in Figures 3 and 4, and the predictions for the interfacial tension and enthalpy of vaporization are shown in Figures 5 and 6. Excellent agreement is found for all of the properties investigated, particularly for the vapour-liquid interfacial tension and enthalpy of vaporisation, which as predictions represent a stringent test of the performance of the model.

The chemical structure of AMP and its proposed SAFT-VR model are presented in Figure 1b). AMP is modelled as a chain molecule with six association sites[84]. As for MEA, two sites of type e and one site of type H are incorporated to account for the association interactions between the hydroxyl group, and one site of type e^* and two sites of type H^* those between the amino group. Given the scarcity of experimental data available for AMP, the physical basis of SAFT is exploited by transferring all of the association parameters from the MEA model previously presented. Hence, only the remaining non-associative parameters (m_{AMP}, $\sigma_{\mathrm{AMP,AMP}}$, $\varepsilon_{\mathrm{AMP,AMP}}$ and $\lambda_{\mathrm{AMP,AMP}}$) need to be estimated from the available experimental data[85–88]. The choice of the final model (see Tables II and IV for the parameter values) was made based on its performance in correlating the VLE data (cf. Figures 3 and 4) and describing the vapour-liquid interfacial tension (cf. Figure 5), although this property was not used in the parameter estimation. Unfortunately, to our knowledge there are no experimental data for the enthalpy of vaporisation of AMP in the open literature.

B. Secondary amines: DEA (transferring association parameters from diethylamine)

In order to gain an understanding of the N-H interaction between secondary amine groups, a SAFT-VR model of diethylamine (DEtA) is developed in the first instance. The chemical structure of DEtA and the correspoding SAFT-VR model are depicted in Figure 1e). Following the general description provided in section II, diethylamine is modelled as a chain molecule with two association sites, one site of type e^* and one site of type H^*. These sites are used to represent the lone pair of electrons on the nitrogen atom and the hydrogen atom on the secondary amine group, respectively. The association scheme we have chosen is consistent with that used in our previous publications[23,51], only e^*-H^* interactions are permitted.

We discretise the parameter space for the model of diethylamine in terms of the dispersive and associative energetic parameters $\varepsilon_{\mathrm{DEtA,DEtA}}$ and $\varepsilon^{HB}_{e^*H^*,\mathrm{DEtA,DEtA}}$ as described in detail in previous work[23,51,75]. The fluid phase equilibrium data are obtained from references[89–92]. An optimal set of SAFT-VR molecular parameters is presented in table I. The comparison of the calculated and experimental VLE data is presented in Figure 2, and the SAFT-VR DFT predictions of the vapour-liquid interfacial tension and enthalpy of vaporisation are presented in Figures 5 and 6, respectively. In this way we have developed a set of parameters which accurately describes the self-association behaviour of a secondary amine group. The physical basis of the SAFT approach is then exploited, and the parameters are transferred to a model of DEA.

Following our previous work on MEA, we propose an asymmetric model of DEA. The chemical structure of DEA and the proposed SAFT-VR model are shown in Figure 1f). The DEA-DEA association is described by including eight association sites to mediate the OH-OH, NH-NH and NH-OH hydrogen-bonding interactions. Two association sites of type e and one of type H are used on each of the hydroxyl functional groups to treat the OH-OH hydrogen-bonding interactions associated with the lone pairs of electrons on the oxygen atoms and hydrogen atoms, respectively. The molecular parameters which describe the OH-OH interactions ($\varepsilon^{HB}_{eH,\mathrm{DEA,DEA}}$ and $r_{c;eH,\mathrm{DEA,DEA}}$) are transferred from the model of ethanol (Table I). A site of type e^* and a site of type H^* are used to represent the amine-amine hydrogen-bonding interactions of the secondary amine group. The molecular parameters which describe the amine-amine hydrogen-bonding interactions of this group ($\varepsilon^{HB}_{e^*H^*,\mathrm{DEA,DEA}}$ and $r_{c;e^*H^*,\mathrm{DEA,DEA}}$) are transferred from the model of diethylamine (Table I). The asymmetric models presented here explicitly acknowledge the fact that the OH-OH (e-H), NH-NH (e^*-H^*) and NH-OH (e-H^* and e^*-H) interactions are distinct from each other. In our model of DEA, only e-H, e^*-H^*, e-H^* and e^*-H site-site interactions are allowed. The procedure of transferring the molecular parameters results in the reduction of the number of parameters that must be estimated from experimental data to eight: m_{DEA}, $\sigma_{\mathrm{DEA,DEA}}$, $\varepsilon_{\mathrm{DEA,DEA}}$, $\lambda_{\mathrm{DEA,DEA}}$, $\varepsilon^{\mathrm{HB}}_{eH^*,\mathrm{DEA,DEA}}$, $\varepsilon^{\mathrm{HB}}_{e^*H,\mathrm{DEA,DEA}}$, $r_{c;e^*H,\mathrm{DEA,DEA}}$ and $r_{c;eH^*,\mathrm{DEA,DEA}}$. Experimental data for the VLE of DEA are obtained from references[89–92]. The optimal set of SAFT-VR molecular parameters used to describe the fluid-phase behaviour of DEA are presented in Tables II and V. A comparison of the calculated and experimental VLE data is presented in Figures 3 and 4, with the predictions of the vapour-liquid interfacial tension and enthalpy of vaporisation presented in Figures 5 and 6, respectively.

C. Tertiary amine compound: MDEA

Methyldiethanolamine (MDEA) also finds applications in CO_2 capture processes. The chemical structure of MDEA and the proposed model for use with SAFT-VR are presented in Figure 1g). Seven sites are included to mediate the hydrogen-bonding interactions of this molecule. We use two sites of type e and one of type H to represent each of the hydroxyl functional groups, with a further site of type e^* representing the lone pair of electrons on the nitrogen atom of the tertiary amine group. Only e-H and e^*-H site-site interactions are permitted in this model. The parameters describing the OH-OH (e-H) hydrogen-bonding interactions ($\varepsilon^{HB}_{eH,\mathrm{MDEA},\mathrm{MDEA}}$ and $r_{c;eH,\mathrm{MDEA},\mathrm{MDEA}}$) are transferred from the model of ethanol[23], reducing the number of parameters which must estimated from the experimental data to six (m_{MDEA}, $\sigma_{\mathrm{MDEA},\mathrm{MDEA}}$, $\varepsilon_{\mathrm{MDEA},\mathrm{MDEA}}$, $\lambda_{\mathrm{MDEA},\mathrm{MDEA}}$, $\varepsilon^{HB}_{e^*H,\mathrm{MDEA},\mathrm{MDEA}}$ and $r_{c;e^*H,\mathrm{MDEA},\mathrm{MDEA}}$). The experimental data used in the estimation procedure can be found in references[90,93,94]. The optimal set of SAFT-VR molecular parameters used to describe the fluid-phase behaviour of MDEA are presented in Tables II and VI. The description of the VLE with SAFT-VR is shown in Figures 3 and 4, with the prediction of the vapour-liquid interfacial tension presented in Figure 5.

IV. AQUEOUS MIXTURES

Binary mixtures of associating compounds are often highly non-ideal, and accurate models are often difficult to develop. Frequently, a number of temperature-dependent binary interaction parameters are required, and assigning values to these parameters can be hampered in the event of insufficient experimental data. In our work, we use experimental VLE data to determine the energetic unlike interaction parameters: ε_{ij} and $\varepsilon^{HB}_{ab,ij}$. All other unlike parameters characterising the binary mixtures (σ_{ij}, λ_{ij} and $r_{c;ab,ij}$) are calculated using arithmetic combining rules of the Lorentz type[9,61].

We build upon previous success in developing an asymmetric model of aqueous mixtures of MEA[23] to develop models for aqueous mixtures of the other multifunctional amines: the unlike interaction parameters which describe the hydrogen bonding interactions between H_2O and the hydroxyl groups on ethanol ($\varepsilon^{HB}_{eH,\mathrm{EtOH},\mathrm{H_2O}}$ and $r_{c;eH,\mathrm{EtOH},\mathrm{H_2O}}$) are transferred to each of the aqueous mixtures of alkanolamines; likewise, the parameters characterising the hydrogen bonding interactions between H_2O and the primary (NH_2) and secondary (NH) amine groups are transferred from models of ethylamine + H_2O and diethylamine + H_2O mixtures, respectively. In this way, we reduce the number of adjustable binary interaction parameters required to describe the fluid-phase behaviour of the asymmetric mixture models to a maximum of one – the unlike dispersion energy parameter (ε_{ij}) in the case of the aqueous MEA, AMP and DEA mixtures, and the unlike hydrogen-bonding interaction ($\varepsilon^{HB}_{e^*H,\mathrm{MDEA,H_2O}}$) in the case of MDEA + H_2O.

A. Aqueous mixtures of primary amines

Three adjustable unlike energy interaction parameters are required to model the MEA + H_2O mixture. The hydrogen bonding energy between water and the hydroxyl group of MEA ($\varepsilon^{HB}_{eH,\mathrm{MEA,H_2O}} = \varepsilon^{HB}_{He,\mathrm{MEA,H_2O}}$) is transferred from that of the mixture of ethanol and water. Since the hydrogen-bonding between water and the amine group of MEA ($\varepsilon^{HB}_{e^*H,\mathrm{MEA,H_2O}} = \varepsilon^{HB}_{H^*e,\mathrm{MEA,H_2O}}$) is also transferred from a model of ethylamine and water, only the unlike dispersion interaction between MEA and water ($\varepsilon_{\mathrm{MEA-H_2O}}$) needs to be estimated from experimental data. Details of the estimation procedure are given in previous work[23]. The binary interaction parameters for the aqueous mixture of MEA are provided in VII. The model describes the mixture behaviour with an accuracy of AAD% = 2.03% in temperature and pressure and AAD = 0.027 in vapour phase composition. The SAFT-VR calculations of isobaric and isothermal slices of the vapour-liquid fluid-phase equilibria for MEA + H_2O are compared with the corresponding experimental data in Figure 7. We note that using our approach, it has been possible to retain a great deal of the microscopic detail characterising the mixture, whilst only utilising one adjustable unlike-interaction parameter to optimise the description of the fluid-phase behaviour.

The interaction parameters for the AMP + H_2O model are obtained in an analogous way: the two different hydrogen-bonding interactions ($\varepsilon^{HB}_{eH,\mathrm{AMP,H_2O}} = \varepsilon^{HB}_{He,\mathrm{AMP,H_2O}}$ and $\varepsilon^{HB}_{e^*H,\mathrm{AMP,H_2O}} = \varepsilon^{HB}_{H^*e,\mathrm{AMP,H_2O}}$) are transferred from models of aqueous mixtures of ethanol and of ethylamine, respectively. As a consequence, only the unlike dispersive interaction ($\varepsilon_{\mathrm{H_2O,AMP}}$) needs to be estimated from VLE experimental data[86]; isobaric data at 0.0667 MPa, 0.08 MPa and 0.1013 MPa are used. The model parameters are given in Table VII, and the comparison of the SAFT-VR description and the experimental data can be seen in Figure 8a). The ADD% = 0.37% in temperature and the AAD = 0.017 in vapour pressure mole fraction.

B. Aqueous mixture of DEA

In order to gain an understanding of the hydrogen-bonding interactions between a secondary amine group (NH) and H_2O, we first consider aqueous mixtures of diethylamine. The unlike interaction energy parameters $\varepsilon_{\mathrm{DEtA,H_2O}}$ and $\varepsilon^{HB}_{e^*H,\mathrm{DEtA,H_2O}}$ are estimated from experimental VLE data[95] at $T = 311.5$ K. The final values of the unlike interaction parameters are presented in Table VII. The theoretical calculations are compared with the experimental data in Figure 8b) at $T = 311.5$ K and 322.25 K. The parameters describing the NH_2-H_2O interaction obtained in this manner for aqueous mixtures of diethylamine are then transferred to the aqueous solutions of DEA.

In modelling a mixture of DEA and H_2O, we transfer the unlike interaction parameters describing the hydrogen-bonding interactions between the hydroxyl group and H_2O and the secondary amine group and H_2O from previous work on EtOH + H_2O and DEtA + H_2O, respectively. Thus, only the value for the unlike dispersion interaction ($\varepsilon_{\mathrm{DEA,H_2O}}$) remains to be estimated from the experimental data[96,97]. The final values of the unlike interaction parameters are presented in Table VII and the corresponding description of the VLE of this mixture is shown in Figure 8c). The coexistence temperature are described with an AAD% = 1.55% and the vapour phase mole fractions an AAD = 0.003.

C. Aqueous mixtures of tertiary amines

In order to gain an understanding of the nature of the hydrogen-bonding interactions between a tertiary amine group and H_2O, we now consider an aqueous mixture of MDEA. We transfer the SAFT-VR model parameters describing the hydrogen-bonding interactions between the hydroxyl groups and water from EtOH+H_2O as we have explained for the other alkanolamines . We are then able to describe accurately the fluid-phase behaviour of the MDEA + H_2O mixture by adjusting only the unlike interaction parameter which characterises the hydrogen bonding between the tertiary amine group and H_2O ($\varepsilon^{HB}_{e^*H,\mathrm{MDEA,H_2O}}$); the unlike dispersion interactions are described well by the value of $\varepsilon_{\mathrm{MDEA,H_2O}}$ given by the Berthelot rule (k_{ij}=0)[61]. Experimental data from Voutsas et al.[98] is employed in the parameter estimation. The final values of the unlike interaction parameters are presented in Table VII and the comparison of the SAFT-VR calculations with the experimental data is shown in Figure 8d). A good agreement is achieved with an AAD% = 2.8% in the coexistence temperature.

V. TERNARY MIXTURES

In the ternary mixtures of alkanolamines, water and carbon dioxide, new species are formed via complex reaction mechanisms[52–55]. The models developed here for use within the SAFT-VR approach describe the phase behaviour of these mixtures without explicitly treating the reactions or the new species. The reactions are instead accounted for with the incorporation of association sites on the CO_2 molecule to mediate the interactions with the amine groups; depending on the alkanolamine and the stoichiometry of the overall reaction, one or two sites are assumed to be active. This implicit treatment of the reactions provides a convenient and straightforward method for the early assessment of new solvents for use in the context of carbon capture processes, as only a limited number of parameters from have to be estimated VLE data to develop the models. It is important to note here that whilst reactions mechanisms or products do not need to be postulated a priori, the SAFT-VR theory can provide valuable information on the degree of speciation of the mixture being studied. This is handled through the analysis of the fraction of sites not bonded (the reader is referred to the SAFT-VR original papers[8,9] for details), and illustrated for the MEA + CO_2 + H_2O system.

There are no experimental data for the binary mixtures of CO_2 and the alkanolamines (MEA, AMP, DEA and MDEA) that are relevant to this investigation. However, VLE data are available for the ternary aqueous mixtures. These data are used to estimate the unlike binary parameters characterising the interactions of CO_2 with the alkanolamines. The unlike binary interaction parameters describing the H_2O + CO_2 mixture are taken from previous work[23] and are included in Table VII for completeness.

A. MEA + CO_2 + H_2O

The MEA + CO_2 + H_2O model proposed here introduces a number of novelties with regard to that presented in earlier work[23]. Firstly, the interaction range of the association sites ($r_{c;ab,\mathrm{MEA},\mathrm{CO_2}}$) is considered as a new adjustable parameter. As a second modification, the interactions between the amino group in the MEA molecule and the two acceptor sites of the CO_2 molecule (labelled α_1 and α_2) are no longer assumed to be characterised by symmetrical parameters (i.e., $\varepsilon^{HB}_{e^*\alpha_1,\mathrm{MEA},\mathrm{CO}_2}$ is not necessarily the same as $\varepsilon^{HB}_{e^*\alpha_2,\mathrm{MEA},\mathrm{CO}_2}$, and neither are $r_{c;e^*\alpha_1,\mathrm{MEA},\mathrm{CO}_2}$ and $r_{c;e^*\alpha_2,\mathrm{MEA},\mathrm{CO}_2}$). Hence, five parameters are now required to describe the MEA + CO_2 binary interactions: $\varepsilon_{\mathrm{MEA},\mathrm{CO}_2}$, $\varepsilon^{HB}_{e^*\alpha_1,\mathrm{MEA},\mathrm{CO}_2}$, $\varepsilon^{HB}_{e^*\alpha_2,\mathrm{MEA},\mathrm{CO}_2}$, $r_{c;e^*\alpha_1,\mathrm{MEA},\mathrm{CO}_2}$ and $r_{c;e^*\alpha_2,\mathrm{MEA},\mathrm{CO}_2}$. Finally, experimental data at high temperatures (up to 393 K) are included in the estimation of the model parameters (previously only data at 313 K were used). We have found that these modifications lead to a marked improvement of the performance of the description of the VLE, particulary at high temperatures. The model parameters are obtained by estimation of the data for five isotherms, ranging from 313 K to 393 K, with a concentration of MEA of 30 wt%[99]. The values of the unlike interaction parameters are presented in Table VIII. A comparison of the SAFT-VR description of the VLE and the experimental data for three isotherms (313 K, 353 K and 393 K) is shown in Figure 9a). The partial pressure of CO_2 is plotted as a function of the CO_2 loading, which is defined as the moles of CO_2 absorbed in the liquid phase per mole of the amine.

The analysis of the degree of speciation for this system at 313 K can be found in Figure 9b). The main equilibrium reactions occurring in this system are the formation of carbamate (MEACOO^-) and bicarbonate (HCO_3^-)[52]. In our model, the concentration of carbamate is equivalent to the concentration of CO_2 molecules bonded at both sites, while the concentration of bicarbonate can be inferred from the concentration of CO_2 molecules with only one bond, given that the model does not allow for CO_2-H_2O or CO_2-CO_2 association,

$$[\mathrm{MEACOO}^-] = x_{\mathrm{CO}_2}[(1 - X_{\alpha_1,\mathrm{CO}_2})(1 - X_{\alpha_2,\mathrm{CO}_2}) \tag{4}$$

$$[\mathrm{HCO}_3^-] = x_{\mathrm{CO}_2}[X_{\alpha_1,\mathrm{CO}_2} + X_{\alpha_2,\mathrm{CO}_2}] \tag{5}$$

where x_{CO_2} is the mole fraction of CO_2 in the liquid phase and $X_{\alpha,i}$ is the fraction of molecules of component i not bonded at the site α. The SAFT-VR predictions for both species are in excellent agreement with the experimental data from Bottinger et al.[100]. For the sake of brevity, these results are only presented for the MEA + CO_2 + H_2O system, although the speciation analysis is general and could be applied to the remainder mixtures.

B. AMP + CO_2 + H_2O

The stoichiometry of the reaction between AMP and CO_2 allows for loadings of up to one molecule of CO_2 per molecule of AMP. To account for this, only one of the acceptor sites of the CO_2 molecule (α_1) is considered to be active (i.e., the interaction energy with the other site is disabled, $\varepsilon^{HB}_{e^*\alpha_2,\mathrm{AMP},\mathrm{CO_2}} = 0$). The reader is directed to previous work[51] for a thorough discussion of this point. Consequently, only three interaction parameters need to be determined for this mixture: $\varepsilon_{\mathrm{AMP},\mathrm{CO_2}}$, $\varepsilon^{HB}_{e^*\alpha_1,\mathrm{AMP},\mathrm{CO_2}}$, and $r_{c;e^*\alpha_1,\mathrm{AMP},\mathrm{CO_2}}$. The VLE for three isotherms (313 K, 333 K and 353 K) at two different concentrations of AMP (17.8 and 35.0 wt%)[101] are used to estimate the model parameters. The optimal values of the parameters are given in Table VIII. A comparison of the calculated phase behaviour and experimental data for AMP concentrations of 17.8 and 35.0 %wt at different temperatures is presented in Figure 10. The agreement is good particularly for low CO_2 loadings and low temperatures; larger deviations are seen for the higher concentration of the amine at higher CO_2 loadings and higher temperatures. We believe this indicates the limits of applicability of the assumption of implicit reactions.

C. DEA + CO_2 + H_2O

The strategy employed for the MEA + CO_2 + H_2O model is found to yield the best results in this case, i.e., the interactions between the amino group of DEA and the two acceptor sites of the CO_2 molecule are not assumed to be described by the same set of parameters. As a consequence, our SAFT-VR description of DEA + CO_2 + H_2O requires the estimation of five parameters, which are determined by simultaneously estimating to five isotherms with temperatures from 298 K to 393 K and DEA concentrations of 20.6, 35.4 and 49.7 wt%[102]. The model parameters are given in Table VIII. The results of the SAFT-VR description can be seen in Figure 11, where one can see a good overall agreement between the calculations and the experimental data, with larger deviations at the higher temperatures.

D. MDEA + CO_2 + H_2O

It is known that MDEA, as a tertiary amine, does not react with CO_2 to form a carbamate, the bicarbonate being formed instead. A detailed discussion of the corresponding reactions in this system has been made by Blauwhoff et al.[52]. The resulting chemical equilibrium results in loadings of up to one molecule of CO_2 per molecule of MDEA being possible, which is accounted for in our SAFT-VR model by considering that only the α_1 site of the CO_2 molecule is active, as for AMP. The three parameters that are required to model the interaction between CO_2 and the amine for MDEA + CO_2 + H_2O are obtained by estimation from experimental data of the VLE for six isotherms with temperatures between 298 K and 413 K and MDEA concentrations ranging from 19 to 53 wt%[103,104]. The model parameters are presented in Table VIII. The adequacy of the SAFT-VR description is apparent from the comparison of the calculated VLE with the experimental data over a range of temperatures for MDEA concentrations of 19, 25 and 32 wt% presented in Figure 12. Figure 12b) constitutes a good example of the predictive capabilities of the SAFT-VR approach, since the experimental data shown[104] have not been used for the parameter estimation.

VI. DISCUSSION AND CONCLUDING REMARKS

We have developed detailed microscopic models for the description of the vapour-liquid equilibria of multifunctional amines that are of interest in the context of CO_2 capture. Our approach preserves a sufficient degree of molecular detail, while minimising the dimensionality of the model parameterization and associated optimisation problem. A key advantage of the SAFT-VR approach is its molecular basis, so that features of the intermolecular interactions of the multifunctional compounds studied here can be transferred from the appropriate groups of related molecules. In modelling MEA, AMP, DEA and MDEA, we have been able to transfer the hydrogen bonding parameters for the hydroxyl-hydroxyl interactions from those of ethanol and those for the amine-amine interactions from ethylamine and diethylamine. As a consequence, only the strength of the amine-hydroxyl hydrogen-bonding interactions for the alkanolamines needs to be determined from pure component VLE data (in addition to the square-well parameters characterising the segment diameters and dispersion energy and range). As has been previously observed[23], the set of molecular parameters which provide the optimal correlation of coexistence data is not necessarily the most physically adequate model. In addition to a correlation of vapour-liquid equilibrium data, we therefore also rely on the ability of the models to provide good predictions of the vapour-liquid interfacial tension and enthalpy of vaporisation; this allows for the discrimination of "optimal" candidate models on a firm physical basis.

These models are used to study the fluid phase equilibria of aqueous solutions of MEA, AMP, DEA and MDEA. The unlike alkanolamine - water association interaction parameters can be transferred from those obtained from aqueous mixtures of ethanol, ethylamine, or diethylamine. In describing these mixtures, we note that only one adjustable, unlike interaction parameter is used: the unlike dispersion interaction energy in the case of the aqueous mixtures of MEA, AMP and DEA; and the hydrogen-bonding energy between the tertiary amine functional group and H_2O in the case of MDEA + H_2O. We emphasise the importance of reducing the number of adjustable parameters required to describe the phase behaviour of these mixtures in light of the fact that these data are often quite scarce, and can be subject to a significant degree of uncertainty.

Finally, the fluid phase behaviour of the reactive aqueous mixtures of alkanolamines and CO_2 is modelled following the approach used in previous work[23,51], to test the applicability of the assumption of implicitly modelling the reaction equilibria with physical models of association. An accurate description of these complex mixtures is of paramount importance for the design and optimisation of carbon capture processes. The stochiometry of the reactions between the alkanolamines and CO_2 is preserved by changing the number of acceptor sites that are active on the CO_2 molecule. The intermolecular model parameters characterising the interaction of these reactive sites on CO_2 with the alkanolamines are determined by estimation using the experimental data of the ternary mixture. Up to five temperature-independent parameters are required to provide a good description of the VLE for some of the mixtures. For some of the amine solvents, the SAFT-VR models can then be used to describe the VLE over large temperature and CO_2 concentration ranges; specifically in the range of interest of operation for absorption/desorption columns. Additionally, predictions of the degree of speciation in the mixture of MEA + CO_2 + H_2O are compared with experimental data of the carbamate and bicarbonate concentrations, and excellent agreement is found. This provides an understanding of the relative proportions of the extent of reaction of CO_2, and supports the case for the use of a physical approach to model the reactions of these systems. In some cases, particulary MEA and AMP, we believe the models could be refined by employing a temperature-dependent unlike association energy (ε_{ij}). Another alternative to improve the description would be to include an explicit treatment of the charged species[21,22], and/or treating the possibility of cooperative association where the association energy depends of the association state of the species[105].

The development of a transferable approach based on the contributions to the free energy of each individual functional group and their interactions is one of the particular strengths of our approach as it provides an adequate representation of the absorption of CO_2 without requiring extensive experimental data. This approach can be seen as an intermediate step toward a full group contribution treatment such as the SAFT-γ approach[106–108]. Our transferable model parameters for primary, secondary, and tertiary alkanolamines, and their aqueous mixtures with CO_2, provide us with a very convenient platform from which to investigate the phase behaviour of other aqueous alkanolamine mixtures of practical and scientific interest, to embark on the challenges inherent in solvent and process design in the context of carbon capture and storage.

VII. ACKNOWLEDGEMENTS

J.R. thanks the Engineering and Physical Sciences Research Council (EPSRC) of the UK for funding to the Molecular Systems Engineering (MSE) group (Grant number: EP/E016340/1) and to the EPSRC and Scottish Power for funding a Knowledge Transfer Partnership. N.M.D is grateful to the British Coal Utilisation and Research Association (BCURA) for the funding of a PhD studentship. Additional funding from BCURA B82, the EPSRC as well as support from the Natural Environment Research Council (NERC) of the UK (Grant number: NE/H01392X/1) is also acknowledged. F.L. thanks Shell for funding a research fellowship.

[1] J. E. McMurry. *Organic Chemistry.* Belmont: Wadsworth, Third edition, 1992.

[2] A. L. Kohl and F. C. Riesenfeld. *Gas Purification.* Gulf Publishing Company, Houston, Texas, Second edition, 1974.

[3] B. Metz, O. Davidson, H. C. de Coninck, M. Loos, and L. A. Meyer. *IPCC, 2006: IPCC Special Report of Carbon Dioxide Capture and Storage. Prepared by Working Group III of the Intergovernmental Panel on Climate Change.* Cambridge University Press, Cambridge, United Kingdom and New York, NY, USA, 2005.

[4] A. B. Rao and E. S. Rubin. A technical, economic and enviromental assessment of amine-based CO_2 capture technology for power plant greenhouse gas control. *Environ. Sci. Technol.*, 36:4467–4475, 2002.

[5] N. Mac Dowell, N. Florin, A. Buchard, J. Hallett, A. Galindo, G. Jackson, C. S. Adjiman, C. K. Williams, N. Shah, and P. Fennell. An overview of CO_2 capture technologies. *Energy Environ. Sci.*, pages 1645–1669, 2010.

[6] H. Herzog. The capture, utilization and disposal of carbon dioxide from fossil fuel-fired power plants. Technical report, Department of Energy, 1993.

[7] A. M. Wolsky, E. J. Daniels, and B. J. Jody. CO_2 capture from the flue gas of conventional fossil fuel fired power plants. *Environ. Prog.*, 13:214–219, 1994.

[8] A. Gil-Villegas, A. Galindo, P. J. Whitehead, S. J. Mills, G. Jackson, and A. N. Burgess. Statistical associating fluid theory for chain molecules with attractive potentials of variable range. *J. Chem. Phys.*, 106:4168–4186, 1997.

[9] A. Galindo, L. A. Davies, A. Gil-Villegas, and G. Jackson. *Mol. Phys.*, 93:241–252, 1998.

[10] P. Paricaud, A. Galindo, and G. Jackson. Recent advances in the use of the SAFT approach in describing electrolytes, interfaces, liquid crystals and polymers. *Fluid Phase Equilib.*, 194:87–96, 2002.

[11] S. P. Tan, H. Adidharma, and M. Radosz. Recent advances and applications of statistical associating fluid theory. *Ind. Eng. Chem. Res.*, 47:8063–8082, 2008.

[12] C. McCabe and A. Galindo. Chapter 8: SAFT associating fluids and fluid mixtures. In *Applied Thermodynamics of Fluids*, pages 215–279. The Royal Society of Chemistry, 2010.

[13] F. Dolezalek. Theory of binary mistures and concentrated solutions. *Z. Phys. Chem.*, 64:727, 1908.

[14] F. Dolezalek. *Z. Phys. Chem.*, 71:191, 1910.

[15] F. Dolezalek. *Z. Phys. Chem.*, 83:47, 1913.

[16] J. J. van Laar. *Z. Phys. Chem.*, 72:723, 1910.

[17] J. J. van Laar. *Z. Phys. Chem.*, 82:599, 1913.

[18] E. D. Eastman and J. Hildebrand. *Am. Chem. Soc.*, 36:2020, 1914.

[19] H. G. Harris and J. M. Prausnitz. *Ind. Eng. Chem. Fundamen.*, 8:180, 1969.

[20] I. G. Economou and M. D. Donohue. Chemical, quasi-chemical and perturbation theories for associating fluids. *AIChE J.*, 37:1875, 1991.

[21] A. Galindo, A. Gil-Villegas, G. Jackson, and A. N. Burgess. SAFT-VRE: Phase behaviour of electrolyte solutions with the statistical associating fluid theory for potentials of variable range. *J. Phys. Chem. B*, 103:10272–10281, 1999.

[22] A. Gil-Villegas, A. Galindo, and G. Jackson. *Mol. Phys.*, 99:531–546, 2001.

[23] N. Mac Dowell, F. Llovell, C. S. Adjiman, G. Jackson, and A. Galindo. Modelling the fluid phase behaviour of carbon dioxide in aqueous solutions of monoethanolamine using transferable parameters with the SAFT-VR approach. *Ind. Eng. Chem. Res.*, 49:1883–1899, 2010.

[24] C. C. Chen, H. I. Britt, J. F. Boston, and L. B. Evans. Local composition model for excess Gibbs energy of electrolyte systems. Part I: Single solvent, single completely dissociated electrolyte systems. *AIChE J.*, 28:588–596, 1982.

[25] C. C. Chen and L. B. Evans. A local composition model for the excess Gibbs energy of aqueous electrolyte systems. *AIChE J.*, 32:444–454, 1986.

[26] D. M Austgen, G. T. Rochelle, X. Peng, and C. C. Chen. Model of vapour-liquid equilibria for aqueous acid gas-alkanolamine systems using the electrolyte-NRTL equation. *Ind. Eng. Chem. Res.*, 28:1060–1073, 1989.

[27] S. Bishnoi and G. T. Rochelle. Physical and chemical solubility of carbon dioxide in aqueous methyldiethanolamine. *Fluid Phase Equilib.*, 168:241–258, 2000.

[28] E. Blanchon le Bouhelec, P. Mougin, A. Barreau, and R. Solimando. Rigorous modeling of the acid gas heat of absorption in alkanolamine solutions. *Energ. Fuel.*, 21:2044–2055, 2007.

[29] G. M. Bollas, C. C. Chen, and P. I. Barton. Refined electrolyte-NRTL model: Activity coefficient expressions for application to multi-electrolyte systems. *AIChE J.*, 54:1608–1624, 2008.

[30] E. T. Hessen, T. Haug-Warberg, and H. F. Svendsen. The refined eNRTL model applied to CO_2-H_2O-alkanolamine systems. *Chem. Eng. Sci.*, 65:3638–3648, 2010.

[31] Y. Song and C. C. Chen. Symmetric electrolyte nonrandom two-liquid activity coefficient model. *Ind. Eng. Chem. Res.*, 48:7788–7797, 2009.

[32] Y. Zhang and C. C. Chen. Thermodynamic modeling for CO_2 absorption in aqueous MDEA solution with electrolyte NRTL model. *Ind. Eng. Chem. Res.*, 50:163–175, 2011.

[33] K. Thomsen, P. Rasmussen, and R. Gani. Correlation and prediction of thermal properties and phase behaviour for a class of aqueous electrolyte systems. *Chem. Eng. Sci.*, 51:3675–3683, 1996.

[34] K. Thomsen and P. Rasmussen. Modeling of vapor-liquid-solid equilibrium in gas-aqueous electrolyte systems. *Chem. Eng. Sci.*, 54:1787–1802, 1999.

[35] L. Faramarzi, G. M. Kontogeorgis, K. Thomsen, and E. H. Stenby. Extended UNIQUAC model for thermodynamic modelling of CO_2 absorption in aqueous alkanolamine solutions. *Fluid Phase Equilib.*, 282:121–132, 2009.

[36] L. Faramarzi, G. M. Kontogeorgis, K. Thomsen, and E. H. Stenby. Thermodynamic modeling of the solubility of CO_2 in aqueous alkanolamine solutions using the extended UNIQUAC

model: Application to monoethanolamine and methyldiethanolamine. *Energy Procedia*, 1:861–867, 2009.

[37] W. Fürst and H. Renon. Representation of excess properties of electrolyte solutions using a new equation of state. *AIChE J.*, 39:335–343, 1993.

[38] G. Vallée, P. Mougin, S. Jullian, and W. Fürst. Representation of CO_2 and H_2S absorption by aqueous solutions of diethanolamine using an electrolyte equation of state. *Ind. Eng. Chem. Res.*, 38:3473–3480, 1999.

[39] L. Chunxi and W. Fürst. Representation of CO_2 and H_2S solubility in aqueous MDEA solutions using an electrolyte equation of state. *Chem. Eng. Sci.*, 55:2975–2988, 2000.

[40] P. J. G. Huttenhuis, N. J. Agrawal, E. Solbraa, and G. F. Versteeg. The solubility of carbon dioxide in aqueous n-methyldiethanolamine solutions. *Fluid Phase Equilib.*, 264:99–112, 2008.

[41] S. H. Huang and M. Radosz. Equations of state for small, large, polydisperse and associating molecules. *Ind. Eng. Chem. Res.*, 29:2284–2294, 1990.

[42] J. K. Button and K. E. Gubbins. SAFT prediction of vapour liquid equilibria of mixtures containing carbon dioxide and aqueous monoethanolamine or diethanolamine. *Fluid Phase Equilib.*, 158:175–181, 1999.

[43] W. G. Chapman, K. E. Gubbins, G. Jackson, and M. Radosz. New reference equation of state for associating liquids. *Ind. Eng. Chem. Res.*, 29:1709–1721, 1990.

[44] A. S. Avlund, G. M. Kontogeorgis, and M. L. Michelsen. Modeling systems containing alkanolamines with the CPA equation of state. *Ind. Eng. Chem. Res.*, 47:7441–7446, 2008.

[45] G. M. Kontogeorgis, E. C. Voutsas, I. V. Yakoumis, and D. P. Tassios. An equation of state for associating fluids. *Ind. Eng. Chem. Res.*, 35:4310–4318, 1996.

[46] A. S. Avlund, D. K. Eriksen, G. M. Kontogeorgis, and M. L. Michelsen. Application of association models to mixtures containing alkanolamines. *Fluid Phase Equilibria*, 306:31–37, 2011.

[47] F. A. Sánchez, A. H. Mohammadi, A. Andreatta, S. Pereda, E. Brignole, and D. Richon. Phase behavior modeling of alkyl amine + hydrocarbon and alkyl amine + alcohol systems using a group contribution associating equation of state. *Ind. Eng. Chem. Res.*, 48:7705–7712, 2009.

[48] F. A. Sánchez, T. M. Soria, S. Pereda, A. H. Mohammadi, D. Richon, and E. A. Brignole. Phase behavior modeling of alkyl-amine+water mixtures and prediction of alkane solubilities

in alkanolamine aqueous solutions with group contribution with association equation of state. *Ind. Eng. Chem. Res.*, 49:7085–7092, 2010.

[49] H. P. Gros, S. Bottini, and E. A. Brignole. A group contribution equation of state for associating mixtures. *Fluid Phase Equilib.*, 116:537–544, 1996.

[50] J. Rozmus, J.-C. de Hemptinne, and P. Mougin. Application of GC-PPC-SAFT EoS to amine mixtures with a predictive approach. *Fluid Phase Equilib.*, 303:15–30, 2011.

[51] N. Mac Dowell, F. E. Pereira, F. Llovell, F. J. Blas, C. S. Adjiman, G. Jackson, and A. Galindo. Transferable SAFT-VR models for the calculation of the fluid phase equilibria in reactive mixtures of carbon dioxide, water and n-alkylamines in the context of carbon capture. *J. Phys. Chem. B.*, 115:8155–8168, 2011.

[52] P. M. M. Blauwhoff, G. F. Versteeg, and W. P. M. van Swaaij. A study on the reaction between CO_2 and alkanolamines in aqueous solutions. *Chem. Eng. Sci.*, 39:207–225, 1984.

[53] P. V. Danckwerts. The reaction of CO_2 with ethanolamines. *Chem. Eng. Sci.*, 34:443–446, 1979.

[54] S. S. Laddha and P. V. Danckwerts. Reaction of CO_2 with ethanolamines: kinetics from gas-absorption. *Chem. Eng. Sci.*, 36:479–482, 1981.

[55] D. E. Penny and T. J. Ritter. Kinetic study of the reactions between carbon dioxide and primary amines. *J. Chem. Soc., Faraday Trans. I.*, 79:2103–2109, 1983.

[56] L. A. Davies, A. Gil-Villegas, and G. Jackson. Describing the properties of chains of segments interacting via soft-core potentials of variable range with the SAFT-VR approach. *Int. J. Thermophys.*, 19:675–686, 1998.

[57] L. A. Davies, A. Gil-Villegas, and G. Jackson. An analytical equation of state for chain molecules formed from Yukawa segments. *J. Chem. Phys.*, 111:8659–8665, 1999.

[58] T. Lafitte, D. Bessieres, M. M. Piñeiro, and J. L. Daridon. Simultaneous estimation of phase behavior and second-derivative properties using the statistical associating fluid theory with variable range approach. *J. Chem. Phys.*, 124:024509, 2006.

[59] C. Avendaño, T. Lafitte, A. Galindo, C. S. Adjiman, G. Jackson, and E. A. Müller. SAFT-γ force field for the simulation of molecular fluids. 1. A single-site coarse grained model of carbon dioxide. *J. Phys. Chem. B*, 115:1154–11169, 2011.

[60] G. Jackson, W. G. Chapman, and K. E. Gubbins. *Mol. Phys.*, 65:1–31, 1988.

[61] J. S. Rowlinson and F. L Swinton. *Liquids and Liquid Mixtures.* Butterworth - Heinemann

Ltd, London, Third edition, 1982.

[62] A. J. Haslam, A. Galindo, and G. Jackson. Prediction of binary intermolecular potential parameters for use in modelling fluid mixtures. *Fluid Phase Equilib.*, 266:105–128, 2008.

[63] W. G. Chapman, G. Jackson, and K. E. Gubbins. *Mol. Phys.*, 65:1057–1079, 1988.

[64] W. G. Chapman, K. E. Gubbins, G. Jackson, and M. Radosz. SAFT: Equation of state solution model for associating fluids. *Fluid Phase Equilib.*, 52:31–38, 1989.

[65] R. Evans. *Fundamentals of Inhomogeneous Fluids, Chapter 3: Density Functionals in the Theory of Nonuniform Fluids*, pages 85–176. Dekker, New York, 1992.

[66] G. J. Gloor, G. Jackson, F. J. Blas, E. M. del Rio, and E. de Miguel. An accurate density functional theory for the vapor-liquid interface of associating chain molecules based on the statistical associating fluid theory for potentials of variable range. *J. Chem. Phys.*, 121:12740–12759, 2004.

[67] G. J. Gloor, G. Jackson, F. J. Blas, E. M. del Rio, and E. de Miguel. Prediction of the vapor-liquid interfacial tension of nonassociating and associating fluids with the SAFT-VR density functional theory. *J. Phys. Chem. C*, 111:15513–15522, 2007.

[68] F. Llovell, A. Galindo, F. J. Blas, and G. Jackson. Classical density functional theory for the prediction of the surface tension and interfacial properties of fluids mixtures of chain molecules based on the statistical associating fluid theory for potentials of variable range. *J. Chem. Phys.*, 133:024704, 2010.

[69] D. A. Fletcher, R. F. McMeeking, and D. Parkin. The United Kingdom Chemical Database Service. *J. Chem. Inf. Comput. Sci.*, 36:746–749, 1996.

[70] J. M. H. Levelt Sengers. Critical exponents at the turn of the century. *Physica*, 82:319–351, 1976.

[71] W. H. Press, S. A. Teukolsky, W. T. Vetterling, and B. P. Flannery. *Numerical Recipes in Fortran.* Cambridge University Press, Cambridge, Second edition, 1992.

[72] F. E. Pereira, G. Jackson, A. Galindo, and C. S. Adjiman. A duality-based optimisation approach for the reliable solution of (P, T) phase equilibrium in volume-composition space. *Fluid Phase Equilib.*, 299:1–23, 2010.

[73] F. E. Pereira, G. Jackson, A. Galindo, and C. S. Adjiman. The HELD algorithm for multicomponent, multiphase equilibrium calculations with generic equations of state. *Comput. Chem. Eng.*, 36:99–118, 2012.

[74] PSE, 2007. http://www.psenterprise.com/, gPROMS v 3.4.

[75] G. N. I. Clark, A. J. Haslam, A. Galindo, and G. Jackson. *Mol. Phys.*, 104:3561–3581, 2006.

[76] M. C. dos Ramos, F. J. Blas, and A. Galindo. Modelling the phase equilibria and excess properties of the water + carbon dioxide binary mixture. *Fluid Phase Equilib.*, 261:359–365, 2007.

[77] M. C. dos Ramos, F. J. Blas, and A. Galindo. Phase equilibria, excess properties, and Henry's constants of the water + carbon dioxide binary mixture. *J. Phys. Chem. C*, 111:15924–15934, 2007.

[78] M. C. dos Ramos. *Phase equilibria of complex mixtures involving supercritical carbon dioxide, water, polymers and surfactants using the SAFT equation of state*. PhD thesis, Universidad de Huelva, 2006.

[79] F. J. Blas and A. Galindo. Study of the high pressure phase behaviour of CO_2+n-alkane mixtures using the SAFT-VR approach with transferable parameters. *Fluid Phase Equilib.*, 194:501–509, 2002.

[80] A. Galindo and F. J. Blas. Theoretical examination of the global fluid phase behaviour and critical phenomena in carbon dioxide + n-alkane binary mixtures. *J. Phys. Chem. B*, 106:4503–4515, 2002.

[81] G. Sartori, W. S. Ho, D. W. Savage, G. R. Chludzinski, and S. Wlechert. Sterically hindered amines for acid-gas absorption. *Sep. and Purif. Rev.*, 16:171–200, 1987.

[82] G. Sartori and D. W. Savage. Sterically hindered amines for CO_2 removal from gases. *Ind. Eng. Chem. Fundam.*, 22:239–249, 1983.

[83] A. Aboudheir, P. Tontiwachwuthikul, and R. Idem. Rigorous model for predicting the behaviour of CO_2 absorption into AMP in packed-bed absorption columns. *Ind. Eng. Chem. Res.*, 45:2553–2557, 2006.

[84] N. Mac Dowell. *The integration of advanced molecular thermodynamics and process modelling for the design of amine-based CO_2 capture processes.* PhD thesis, Imperial College London, 2010.

[85] A. Barreau, P. Mougin, C. Lefebvre, Q. M. Luu Thi, and J. Rieu. Ternary isobaric vapor liquid equilibria of methanol + n-methyldiethanolamine + water and methanol + 2-amino-2-methyl-1-propanol + water systems. *J. Chem. Eng. Data*, 53:613–613, 2008.

[86] G. D. Pappa, C. Anastasi, and E. C. Voutsas. Measurement and thermodynamic modelling of

the phase equilibrium of aqueous 2-amino-2-methyl-1-propanol solutions. *Fluid Phase Equilib.*, 243:193–197, 2006.

[87] S. Xu, F. D. Otto, and A. E. Mather. Physical properties of aqueous AMP solutions. *J. Chem. Eng. Data*, 36:71–75, 1991.

[88] A. Zúñiga-Moreno, L. A. Galicia-Luna, J. M. Bernal-García, and G. A. Iglesias-Silva. Densities and derived thermodynamic properties of 2-amino-2-methyl-1-propanol + water mixtures at temperatures from 313 to 363 K and pressures up to 24 MPa. *J. Chem. Eng. Data*, 53:100–107, 2008.

[89] S. Horstmann, P. Mougin, F. Lecomte, K. Fischer, and J. Gmehling. Phase equilibrium and excess enthalpy data for the system methanol + 2,2-diethanolamine + water. *J. Chem. Eng. Data*, 47:1496–1501, 2002.

[90] O. Noll, A. Valtz, D. Richon, T. Getachew-Sawaya, L. Mokbel, and J. Jose. Vapor pressure and liquid densities of n-methylethanolamine, diethanolamine, and n-methyldiethanolamine. *J. Chem. Eng. Data*, 3:105–120, 1998.

[91] R. M. DiGuilio, R. J. Lee, S. T. Schaeffer, L. L. Brasher, and A. S. Teja. Densities and viscosities of the ethanolamines. *J. Chem. Eng. Data*, 37:239–242, 1992.

[92] F. Murrieta-Guevara and A. Trejo Rodríguez. Liquid density as a function of temperature of five organic solvents. *J. Chem. Eng. Data*, 29:204–206, 1984.

[93] T. E. Daubert. DIPPR Data Series 2, AIChE : New York. pages 143–153, 1994.

[94] J. M. Bernal-García, M. Ramos-Estrada, G. A. Iglesias-Silva, and K. R. Hall. Densities and excess molar volumes of aqueous solutions of n-methyldiethanolamine (MDEA) at temperatures from 283.15 to 363.15 K. *J. Chem. Eng. Data*, 48:1442–1445, 2003.

[95] M. Hirata, S. Ohe, and K. Nagahama. *Computer aided data book of vapor-liquid equilibria*. Kodansha limited, Tokyo, and Elsevier scientific Publishing Company, Amsterdam, Oxford, and New York, 1976.

[96] Z. Cai, R. Xie, and Z. Wu. Binary isobaric vapor-liquid equilibria of ethanolamines + water. *J. Chem. Eng. Data*, 41:1101–1103, 1996.

[97] M. Abedinzadegan Abdi and A. Meisen. A novel process for diethanolamine recovery from partially degraded solutions. 1. Process description and phase equilibria of the DEA-BHEP-THEED-hexadecane system. *Ind. Eng. Chem. Res.*, 38:3096–3104, 1999.

[98] E. Voutsas, A. Vrachnos, and K. Magoulas. Measurement and thermodynamic modeling of

the phase equilibrium of aqueous n-methyldiethanolamine solutions. *Fluid Phase Equilib.*, 224:193–197, 2004.

[99] F. Y. Jou, A. E. Mather, and F. D. Otto. The solubility of CO_2 in a 30 mass percent monoethanolamine solution. *Can. J. Chem. Eng.*, 73:140–147, 1995.

[100] W. Böttinger, M. Maiwald, and H. Hasse. Online NMR spectroscopic study of species distribution in MEA-H_2O-CO_2 and DEA-H_2O-CO_2. *Fluid Phase Equilib.*, 263:131–143, 2008.

[101] D. Silkenbaumer, B. Rumpf, and R. N. Lichtenthaler. Solubility of carbon dioxide in aqueous solutions of 2-amino-2-methyl-1-propanol and n-methyldiethanolamine and their mixtures in the temperature range from 313 to 353 K and pressures up to 2.7 MPa. *Ind. Eng. Chem. Res.*, 37:3133–3141, 1998.

[102] J. I. Lee, F. D. Otto, and A. E. Mather. Solubility of carbon dioxide in aqueous diethanolamine solutions at high pressures. *J. Chem. Eng. Data*, 17:465–468, 1972.

[103] G. Kuranov, B. Rumpf, N. A. Smirnova, and G. Maurer. Solubility of single gases carbon dioxide and hydrogen sulfide in aqueous solutions of n-methyldiethanolamine in the temperature range 313-413 K at pressures up to 5 MPa. *Ind. Eng. Chem. Res.*, 35:1959–1966, 1996.

[104] R. Sidi-Boumedine, S. Horstmann, K. Fischer, E. Provost, W. Fürst, and J. Gmehling. Experimental determination of carbon dioxide solubility data in aqueous alkanolamine solutions. *Fluid Phase Equilib.*, 218:85–94, 2004.

[105] R. P. Sear and G Jackson. Thermodynamic perturbation theory for association with bond cooperativity. *J. Chem. Phys.*, 105:1113–1120, 1996.

[106] A. Lymperiadis, C. S. Adjiman, A. Galindo, and G. Jackson. A group contribution method for associating chain molecules based on the statistical associating fluid theory (SAFT-γ). *J. Chem. Phys.*, 127:234903, 2007.

[107] A. Lymperiadis, C. S. Adjiman, G. Jackson, and A. Galindo. A generalisation of the SAFT-γ group contribution method for groups comprising multiple spherical segments. *Fluid Phase Equilib.*, 274:85–104, 2008.

[108] V. Papaioannou, C. S. Adjiman, G. Jackson, and A. Galindo. Simultaneous prediction of vapour-liquid and liquid-liquid equilibria (VLE and LLE) of aqueous mixtures with the SAFT-γ group contribution approach. *Fluid Phase Equilib.*, 306:82–96, 2011.

Table I: The parameters characterising the pure component intermolecular potential models of ethanol, ethylamine, diethylamine, water and carbon dioxide: the number of segments m_i, the diameter of the spherical core σ_{ii}, the depth ε_{ii}, and range λ_{ii} of the dispersive square well, the number of each type of association sites. The percentage AADs for vapor pressure (AAD% P) and liquid density (AAD% ρ) are employed to assess the quality of the description. All like site-site interactions are equal to zero ($\varepsilon^{HB}_{ee,ii} = \varepsilon^{HB}_{HH,ii} = \varepsilon^{HB}_{\alpha\alpha,ii} = 0$).

i	m_i	σ_{ii}(Å)	ε_{ii}/k(K)	λ_{ii}	e-sites	H-sites	α_1-sites	α_2-sites	$\varepsilon^{HB}_{eH,ii}/k$(K)	$r_{c;eH,ii}$(Å)	AAD% P	AAD% ρ
EtOH	1.533	3.71500	244.417	1.67300	2	1	0	0	2357.79	2.17328	6.75	0.4
$EtNH_2$	1.666	3.67397	960.000	1.55757	1	1	0	0	780.000	2.71709	1.08	0.22
DEtA	2.347	3.80766	250.000	1.55757	1	1	0	0	780.000	2.71709	0.64	0.93
H_2O	1.0	3.03420	250.000	1.78890	2	2	0	0	1400.00	2.10822	0.69	0.98
CO_2	2.0	2.7864	179.270	1.51573	0	0	1	1	-	-	0.61	1.18

Table II: The parameters characterising the pure component intermolecular potential models of MEA, AMP, DEA and MDEA (the number of segments m_i, the diameter of the spherical core σ_{ii}, the depth ε_{ii} and range λ_{ii} of the dispersive square well and number and type of association sites). The percentage absolute average deviation AAD%, and separate percentage AADs for vapor pressure (AAD% P) and liquid density (AAD% ρ) are employed to assess the quality of the description. All like site-site interactions are equal to zero ($\varepsilon^{HB}_{ee,ii} = \varepsilon^{HB}_{HH,ii} = \varepsilon^{HB}_{e^*e^*,ii} = \varepsilon^{HB}_{H^*H^*,ii} = 0$). Note that the sites of the amino groups e and H refer to e^* and H^* in the text.

i	m_{ii}	σ_{ii} (Å)	ε_{ii}/k(K)	λ_{ii}	e-sites	H-sites	e^*-sites	H^*-sites	AAD%	AAD% P	AAD% ρ
MEA	2	3.57229[a]	305.000	1.58280	2	1	1	1	2.41	3.58	0.26
AMP	2.29	3.99053	328.065	1.48043	2	1	1	2	0.29	0.6	0.07
DEA	2.71	3.72439	211.378	1.59433	4	2	1	1	1.87	4.99	0.11
MDEA	2.49	4.03836	210.106	1.75471	4	2	1	0	0.47	3.65	0.1

[a] In our previous work, a value of 3.52779 was erroneously given.

Table III: The site-site association energies $\varepsilon^{HB}_{ab,\text{MEA,MEA}}$ and range parameter $r_{c;ab,\text{MEA,MEA}}$ for the asymmetric model of MEA (Figure 1a).

	$\varepsilon^{HB}_{ab,\text{MEA,MEA}}/k$ (K)				$r_{c;ab,(\text{MEA})}$ (Å)			
$b\backslash a$	e	H	e^*	H^*	e	H	e^*	H^*
e	0	2357.79	0	900.00	0	2.08979	0	2.65064
H	2357.79	0	550.00	0	2.08979	0	2.65064	0
e^*	0	550.00	0	960.00	0	2.65064	0	2.32894
H^*	900.0	0	960.00	0	2.65064	0	2.32894	0

Table IV: The site-site association energies $\varepsilon^{HB}_{ab,\mathrm{AMP,AMP}}$ and range parameter $r_{c;ab,\mathrm{AMP,AMP}}$ for the asymmetric model of AMP (Figure 1b).

	$\varepsilon^{HB}_{ab,\mathrm{AMP,AMP}}/k$ (K)				$r_{c;ab,\mathrm{AMP,AMP}}$ (Å)			
$b\backslash a$	e	H	e^*	H^*	e	H	e^*	H^*
e	0	2357.79	0	900.00	0	2.33446	0	2.96097
H	2357.79	0	550.00	0	2.33446	0	2.96097	0
e^*	0	550.00	0	960.00	0	2.96097	0	2.60161
H^*	900.00	0	960.00	0	2.96097	0	2.60161	0

Table V: The site-site association energies $\varepsilon^{HB}_{ab,\mathrm{DEA,DEA}}$ and range parameter $r_{c;ab,\mathrm{DEA,DEA}}$ for the asymmetric model of DEA (Figure 1f).

	$\varepsilon^{HB}_{ab,\mathrm{DEA,DEA}}/k$ (K)				$r_{c;ab,\mathrm{DEA,DEA}}$ (Å)			
$b\backslash a$	e	H	e^*	H^*	e	H	e^*	H^*
e	0	2357.79	0	1093.39	0	2.17877	0	3.28006
H	2357.79	0	2737.90	0	2.17877	0	2.62856	0
e^*	0	2737.90	0	780.00	0	2.62856	0	2.65771
H^*	1093.39	0	780.00	0	3.28006	0	2.65771	0

Table VI: The site-site association energies $\varepsilon^{HB}_{ab,\mathrm{MDEA,MDEA}}$ and range parameter $r_{c;ab,\mathrm{MDEA,MDEA}}$ for the asymmetric model of MDEA (Figure 1g).

	$\varepsilon^{HB}_{ab,\mathrm{MDEA,MDEA}}/k$ (K)			$r_{c;ab,\mathrm{MDEA,MDEA}}$(Å)		
$b\backslash a$	e	H	e^*	e	H	e^*
e	0	2357.79	0	0	2.36244	0
H	2357.79	0	1689.88	2.36244	0	3.31205
e^*	0	1689.88	0	0	3.31205	0

Table VII: Binary interaction parameters for aqueous mixtures of MEA, AMP, DEA, MDEA, EtOH, $EtNH_2$, DEtA and CO_2. Here, ε_{ij} characterises the strength of the dispersion interaction between molecules of types i and j, and $\varepsilon^{HB}_{ab,ij}$ and $r_{c,ab,ij}$ the strength and range of the association between sites a and b of molecules i and j. The unlike association between sites of the same type is assumed to be symmetric, i.e., $\varepsilon^{HB}_{eH,ij} = \varepsilon^{HB}_{He,ij}$ and $\varepsilon^{HB}_{e^*H,ij} = \varepsilon^{HB}_{H^*e,ij}$.

i	+ j	ε_{ij}/k(K)	$\varepsilon^{HB}_{eH,ij}/k$(K)	$\varepsilon^{HB}_{e^*H,ij}/k$(K)	$r_{c;eH,ij}$(Å)	$r_{c;e^*H,ij}$(Å)
MEA	+ H_2O	273.373	1780.71	1517.10	2.10763 [a]	2.22626[b]
AMP	+ H_2O	292.733	1780.71	1517.10	2.21340	2.33264
DEA	+ H_2O	275.855	1780.71	1250.00	2.14735	2.39142
MDEA	+ H_2O	229.187	1780.71	1800.00	2.22547	2.71327
EtOH	+ H_2O	252.870	1780.71	0	2.14374	0
$EtNH_2$	+ H_2O	277.690	0	1517.11	0	2.25215
DiEtNH	+ H_2O	292.500	0	1250.00	0	2.41273
CO_2	+ H_2O	224.404	0	0	0	0

[a] In our previous work, a value of 2.14374 was erroneously given.

[b] In our previous work, a value of 2.25215 was erroneously given.

Table VIII: Binary interaction parameters for the mixtures of MEA, AMP, DEA, MDEA with CO_2. Here, ε_{ij} characterises the strength of the dispersion interaction between molecules of types i and j, and $\varepsilon^{HB}_{ab,ij}$ and $r_{c,ab,ij}$ the strength and range respectively of the association between sites a and b of molecules i and j. The unlike association between sites of the same type is assumed to be symmetric, i.e., $\varepsilon^{HB}_{ab,ij} = \varepsilon^{HB}_{ba,ij}$.

i	+ j	ε_{ij}/k	$\varepsilon^{HB}_{e^*\alpha_1,ij}/k$(K)	$\varepsilon^{HB}_{e^*\alpha_2,ij}/k$(K)	$r_{c;e^*\alpha_1,ij}$(Å)	$r_{c;e^*\alpha_2,ij}$(Å)
MEA	+ CO_2	121.87	5200.0	3982.66	1.97978	1.96999
AMP	+ CO_2	153.71	6405.9	0	1.80000	0
DEA	+ CO_2	160.64	4448.2	5862.64	1.85000	1.85000
MDEA	+ CO_2	121.46	6253.0	0	1.85700	0

Figure 1: Chemical formulae and schematic representation of the SAFT-VR molecular models for the compounds studied in this work. Different association site types are represented by different labels (e, e^*, H, H^*, α_1, and α_2). a) MEA, b) AMP, c) $\mathrm{EtNH_2}$, d) EtOH, e) DEtA, f) DEA, g) MDEA, h) H_2O, and i) CO_2.

Figure 2: Experimental data (symbols) for $\mathrm{EtNH_2}$, EtOH and DEtA are compared with the calculated values obtained using the proposed models (continuous curves) with the SAFT-VR equation-of-state: a) Saturated vapor pressures. The Clausius-Clapeyron representation is presented, as the low temperature region is more easily observed in this projection. b) Coexistence densities.

Figure 3: Clausius-Clapeyron representation of the experimental saturated vapour pressures (symbols) for a) MEA, b) AMP, c) DEA and d) MDEA compared to the calculated values obtained using the proposed models (continuous curves) with the SAFT-VR equation-of-state.

Figure 4: Experimental coexistence densities ρ (symbols), for MEA, AMP, DEA and MDEA are compared with the calculated values obtained using the proposed models (continuous curves) with the SAFT-VR equation-of-state.

Figure 5: Experimental vapour-liquid interfacial tensions γ (symbols) of a) MEA, b) AMP, c) DEA, d) MDEA, e) DEtA and f) $\mathrm{EtNH_2}$ are compared with the predicted values obtained using the proposed models (continuous curves) with the SAFT-VR DFT approach[66–68]. The predictions for the interfacial tension are presented for all the compounds for which experimental data[69] is available.

Figure 6: Experimental enthalpies of vaporisation, ΔH_{fg}, (symbols)[69] of a) MEA, b) DEA and c) DiEtNH are compared with the predicted values obtained using the proposed models (continuous curves) with the SAFT-VR approach.

Figure 7: a) Isobaric temperature-composition Tx slices of vapour-liquid equilibrium of an aqueous mixture of MEA at pressures of 0.2242 MPa (red squares), 0.1013 MPa (black diamonds) and 0.06666 MPa (blue circles). b) Isothermal pressure-composition Px slices of vapour-liquid equilibrium of an aqueous mixture of MEA at temperatures of 298 K (red

squares), 343 K (black diamonds) and 364 K (blue circles). The symbols correspond to the experimental[69] data and the curves to the SAFT-VR calculations.

Figure 8: a) Isobaric temperature-composition Tx slices of the vapour-liquid equilibrium of an aqueous mixture of AMP at pressures of 0.101 MPa (red squares), 0.08 MPa (black diamonds) and 0.0667 MPa (blue circles). b) Isothermal pressure-composition Px slices of the vapour-liquid equilibrium of diethylamine and water at T = 311.5 K (black diamonds) and T = 322.25 K (red squares). c) Isobaric temperature-composition Tx slices of the vapour-liquid equilibrium of an aqueous mixture of DEA at P = 0.007 MPa (black diamonds) and P = 0.0267 MPa (red squares). d) Isobaric temperature-composition Tx slices of the vapour-liquid equilibrium of an aqueous mixture of MDEA at P = 0.0399 MPa (blue circles), P = 0.0533 MPa (black diamonds), and P = 0.0667 MPa (red squares). The symbols correspond to the experimental data[86,95–98] and the curves to the SAFT-VR calculations.

Figure 9: a) Isotherms of projections of the pressure-loading vapour-liquid equilibrium of the ternary mixture MEA + H_2O + CO_2 with a concentration of MEA in the liquid phase of 30 wt% , at T = 313 K, T = 353 K, and T = 393 K. b) Predicted mole fraction of carbamate and bicarbonate in the ternary mixture of MEA + H_2O + CO_2 with a concentration of MEA in the liquid phase of 30 wt% , at T = 313 K. The symbols (blue squares for carbamate and red diamonds for bicarbonate) correspond to the experimental data[99,100] and the curves (continuous blue line for carbamate and dashed red line for bicarbonate) to the SAFT-VR calculations. The CO_2 loading (θ_{CO_2}) is defined as the moles of CO_2 absorbed in the liquid phase per mole of the amine.

Figure 10: Isotherms of projections of the pressure-loading vapour-liquid equilibrium of the ternary mixture AMP + H_2O + CO_2, at T = 313 K, T = 333 K, and T = 353 K. a) Concentration of AMP in the liquid phase of 17 wt%. b) Concentration of AMP in the liquid phase of 35 wt%. The symbols correspond to the experimental data[101] and the curves to the SAFT-VR calculations.

Figure 11: Isotherms of projections of the pressure-loading vapour-liquid equilibrium of the ternary mixture DEA + H_2O + CO_2, at T = 298 K, T = 323 K, T = 348 K, T =

373 K, and T = 393 K. a) Concentration of DEA in the liquid phase of 20.6 wt%. b) Concentration of DEA in the liquid phase of 35.4 wt%. The symbols correspond to the experimental data[102] and the curves to the SAFT-VR calculations.

Figure 12: Isotherms of projections of the pressure-loading vapour-liquid equilibrium of the ternary mixture MDEA + H_2O + CO_2. The symbols correspond to the experimental data[103,104] and the curves to the SAFT-VR calculations. a) Concentration of MDEA in the liquid phase of 19 wt% at T = 313 K, T = 333 K, T = 373 K, T = 393 K, and T = 413K. c) Concentration of MDEA in the liquid phase of 25 wt% at T = 313 K and T = 348 K. These calculations are predictions, as these experimental data have not been used in the parameter estimation. b) Concentration of MDEA in the liquid phase of 32 wt% at T = 313 K, T = 333 K, T = 373 K, T = 393K, and T = 413K.

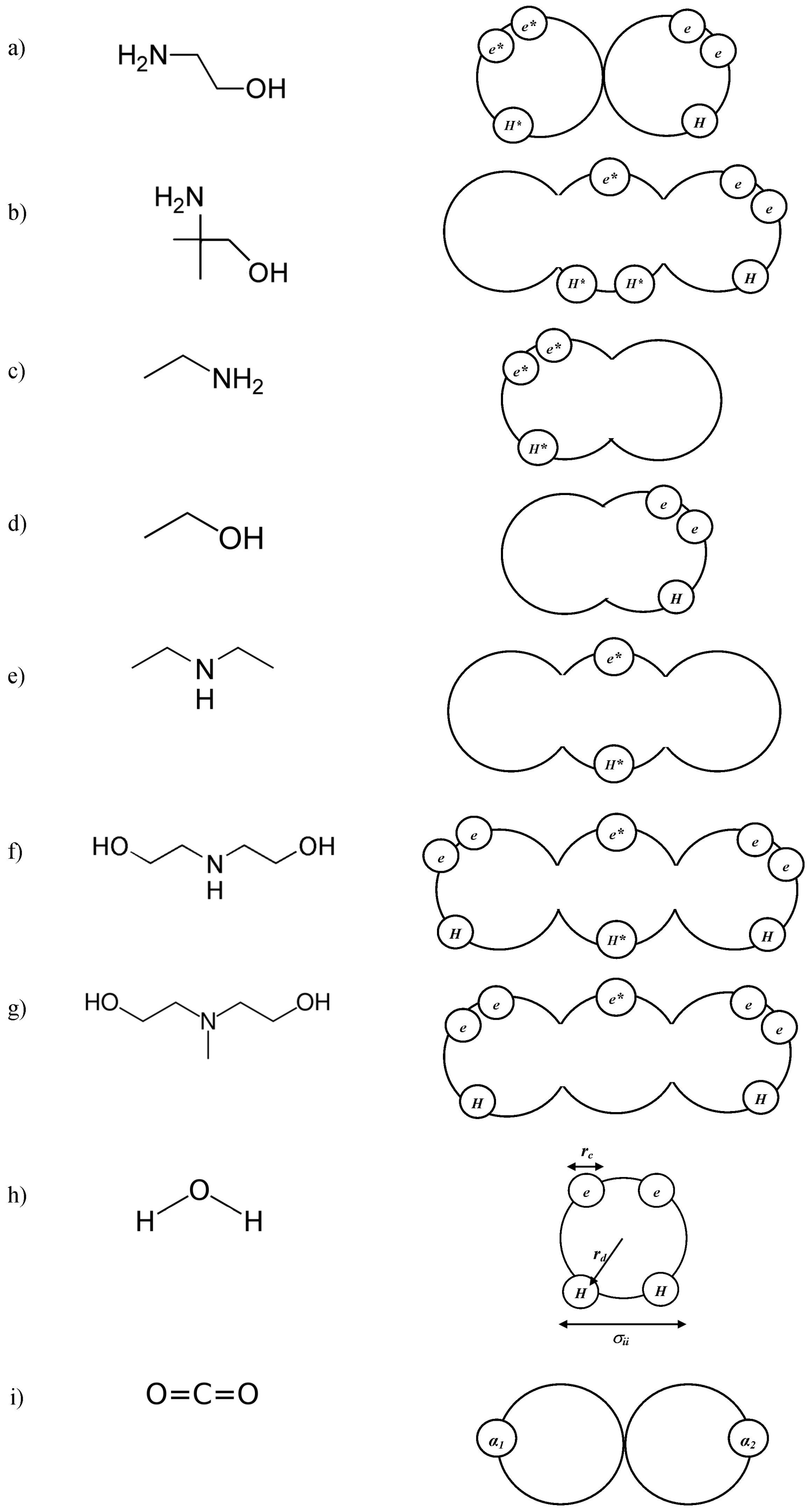
a)
H2N
OH
e*
e*
H*
e
e
H
b)
H2N
OH
e*
e
e
H*
H*
H
c)
NH2
e*
e*
H*
d)
OH
e
e
H
e)
N
H
e*
H*
f)
HO
N
H
OH
e
e
e*
e
e
H
H*
H
g)
HO
N
OH
e
e
e*
e
e
H
H
h)
O
H
H
r_c
e
e
r_d
H
H
σ_ii
i)
O=C=O
α1
α2

Figure 1:

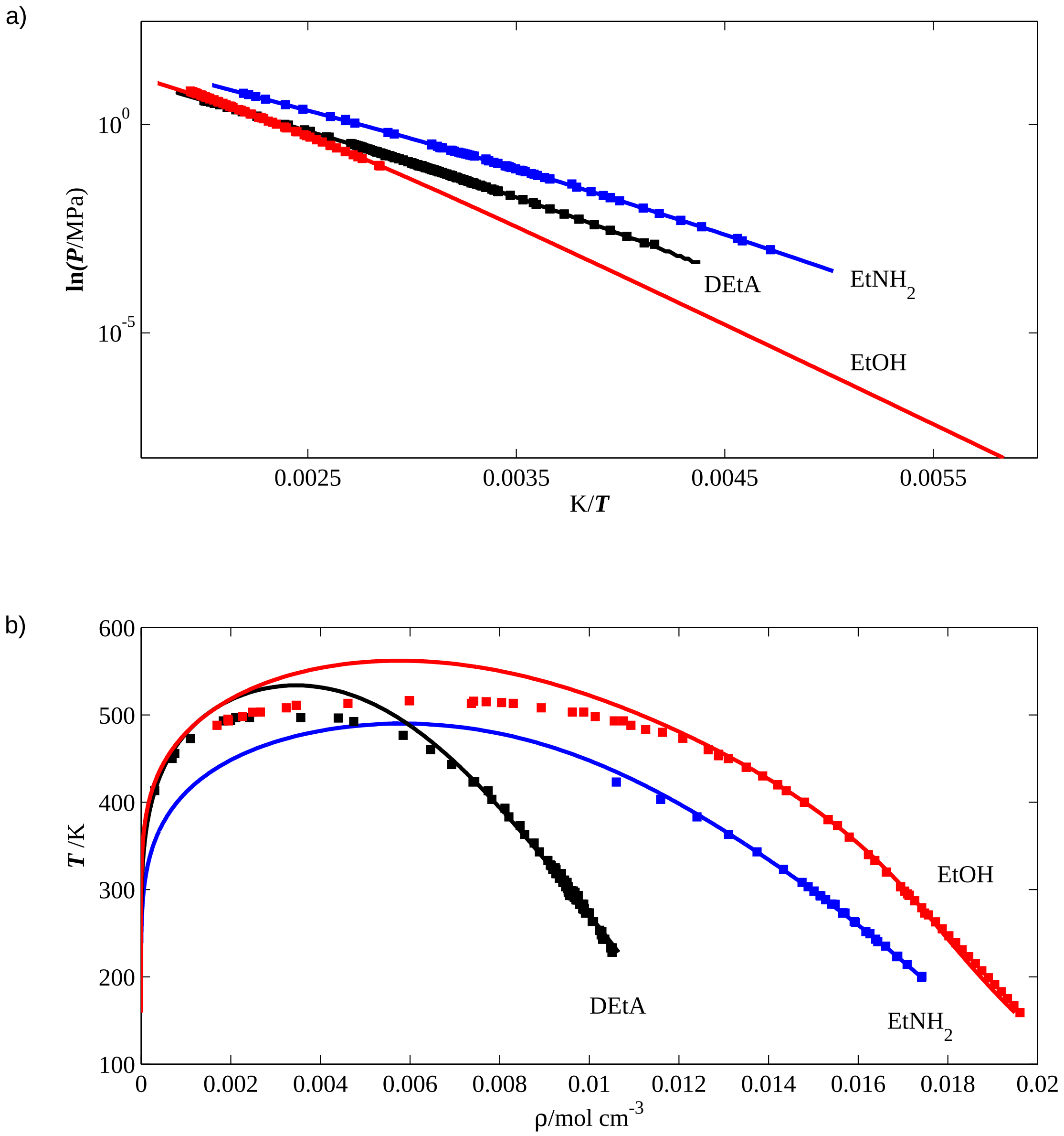
a)
10^0
10^-5
ln(P/MPa)
0.0025
0.0035
0.0045
0.0055
K/T
DEtA
EtNH2
EtOH
b)
600
500
400
300
200
100
T /K
0
0.002
0.004
0.006
0.008
0.01
0.012
0.014
0.016
0.018
0.02
ρ/mol cm-3
DEtA
EtNH2
EtOH

Figure 2:

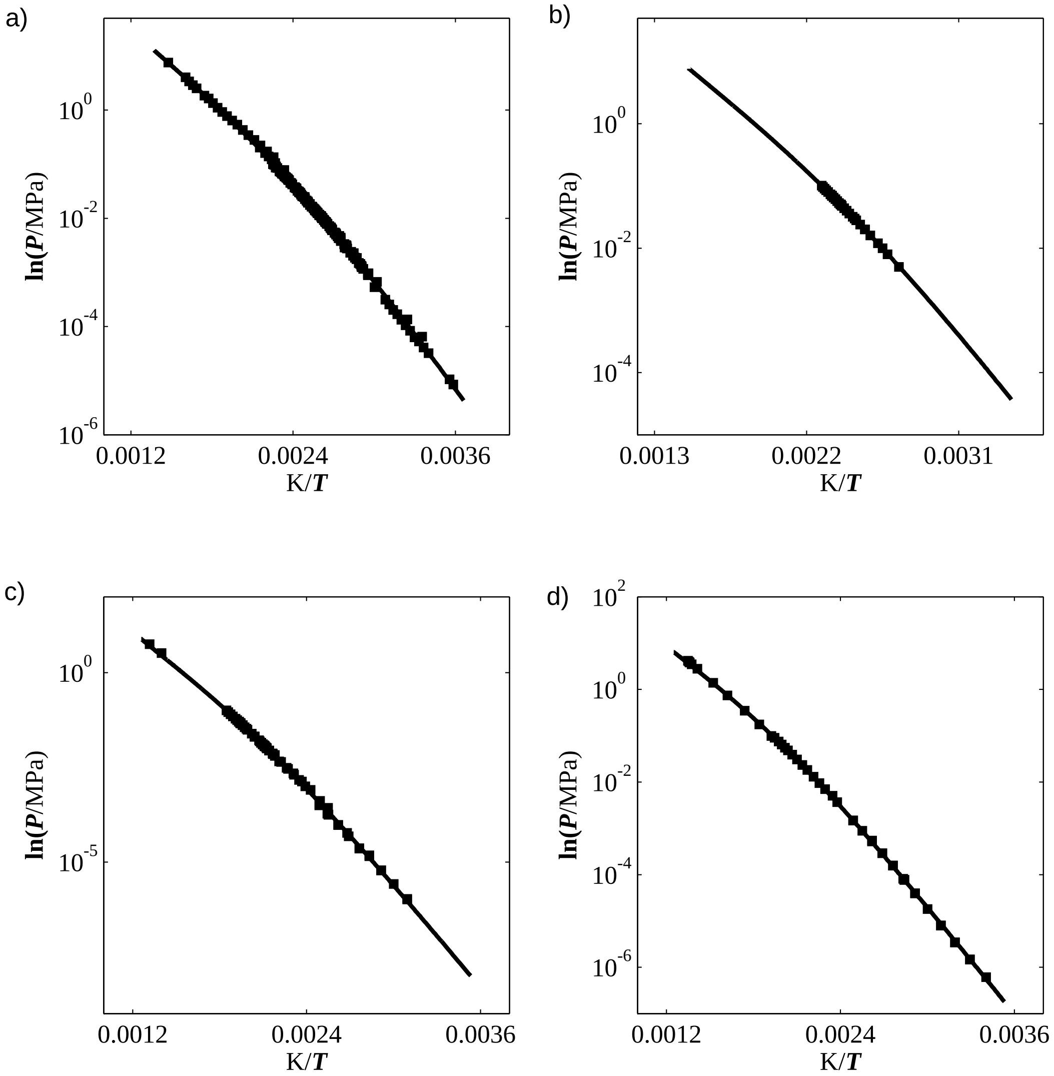
a)
b)
c)
d)
ln(P/MPa)
K/T
10^0
10^-2
10^-4
10^-6
0.0012
0.0024
0.0036
10^0
10^-2
10^-4
0.0013
0.0022
0.0031
10^0
10^-5
0.0012
0.0024
0.0036
10^2
10^0
10^-2
10^-4
10^-6
0.0012
0.0024
0.0036

Figure 3:

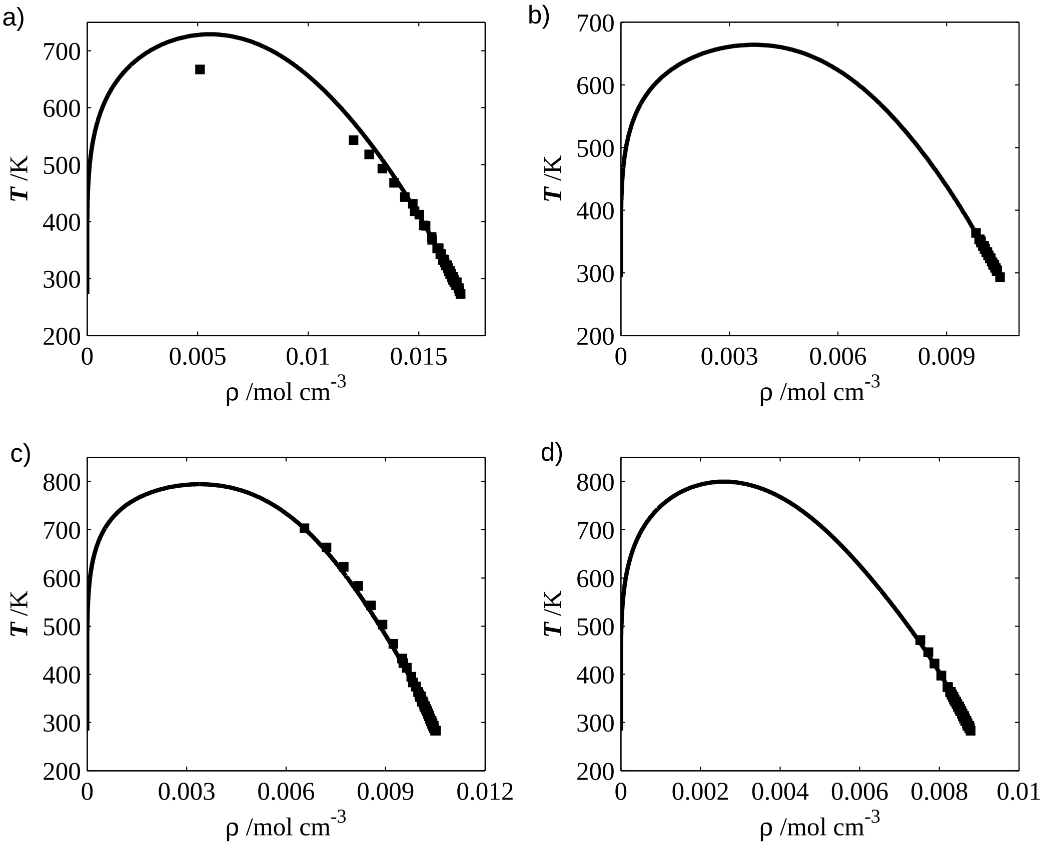
a)
b)
c)
d)
T /K
ρ /mol cm^{-3}
200
300
400
500
600
700
800
0
0.005
0.01
0.015
0.002
0.003
0.004
0.006
0.008
0.009
0.012

Figure 4:

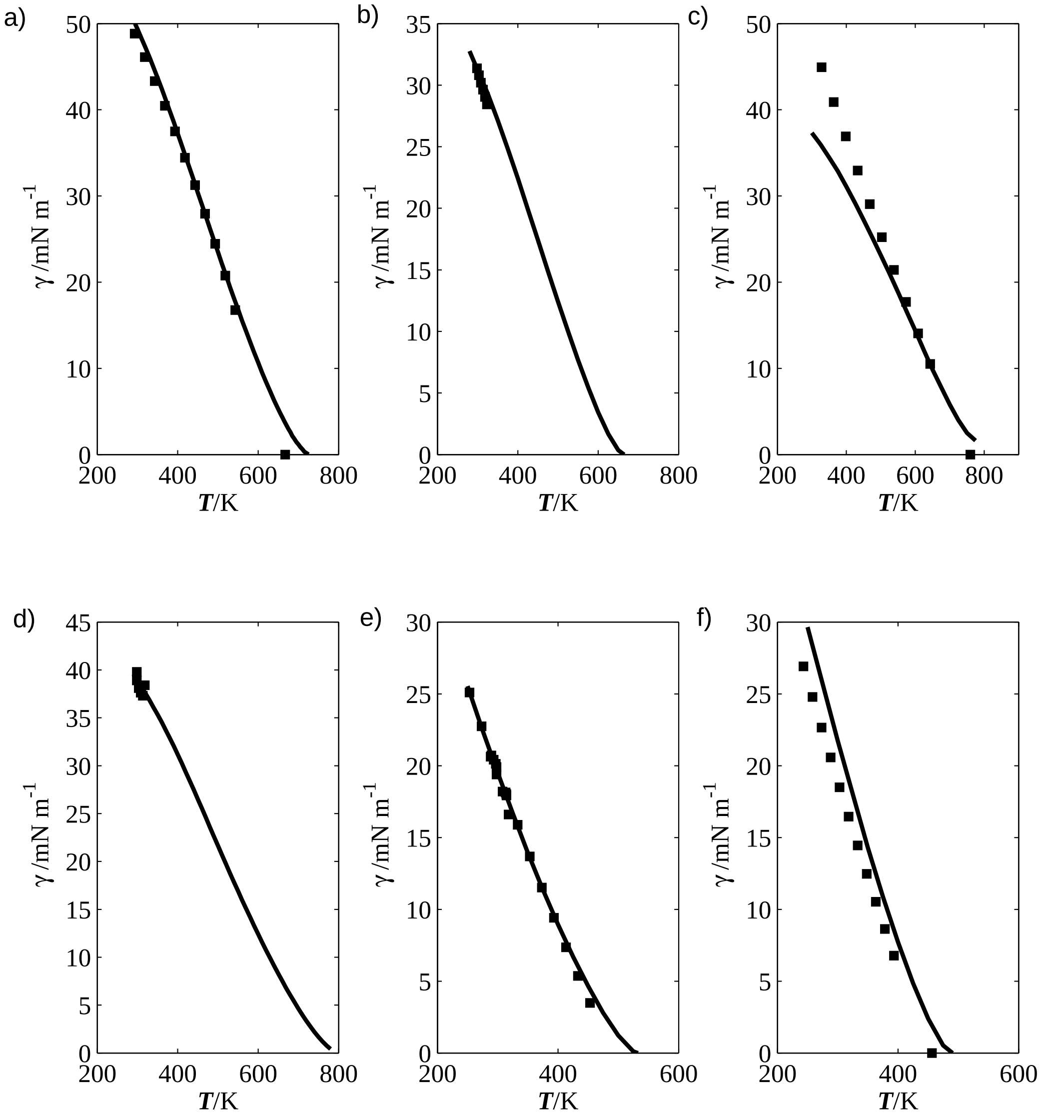

Figure 5:

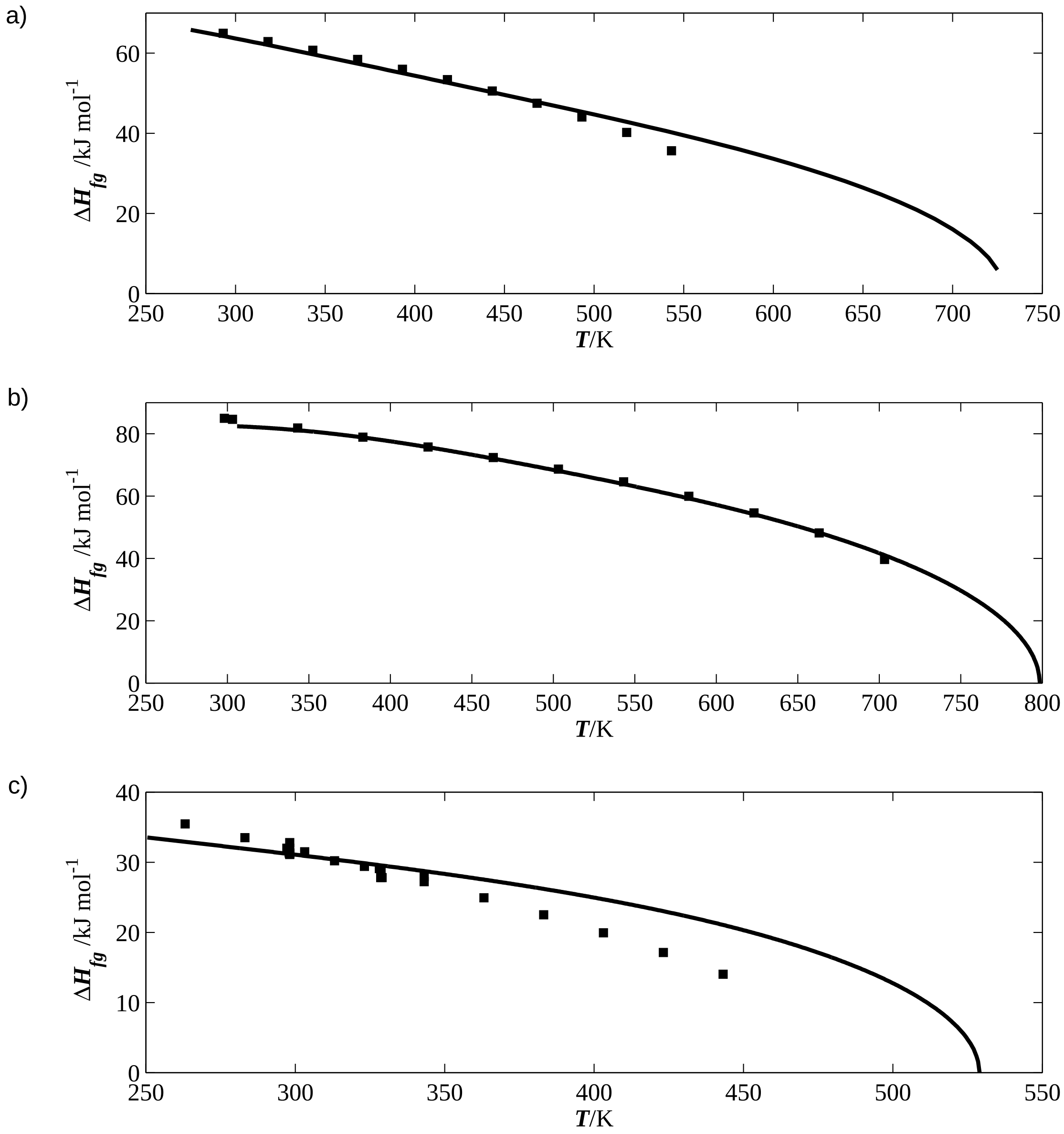
a)
60
40
20
0
ΔH_fg /kJ mol-1
250
300
350
400
450
500
550
600
650
700
750
T/K
b)
80
60
40
20
0
ΔH_fg /kJ mol-1
250
300
350
400
450
500
550
600
650
700
750
800
T/K
c)
40
30
20
10
0
ΔH_fg /kJ mol-1
250
300
350
400
450
500
550
T/K

Figure 6:

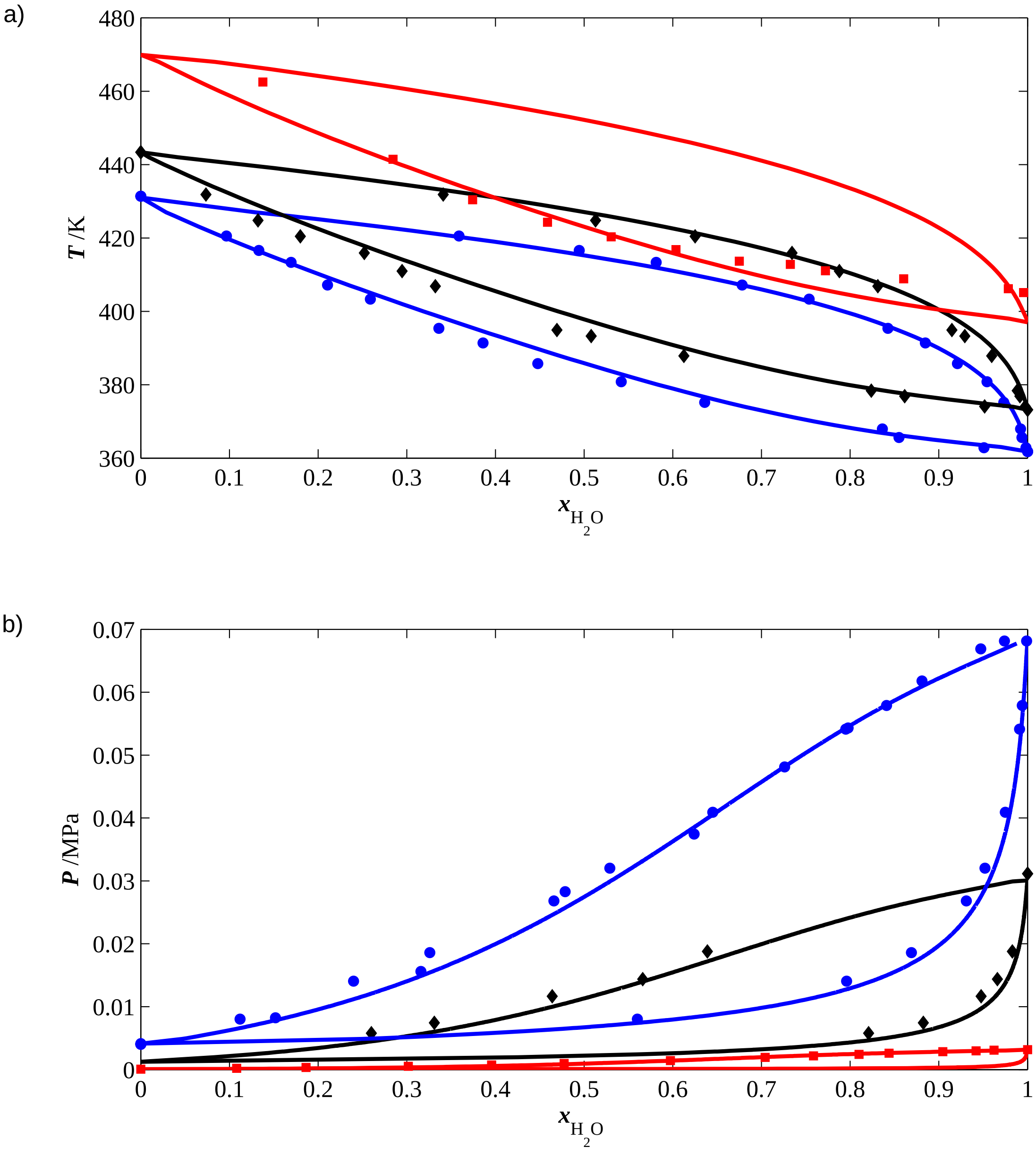
a)
480
460
440
420
400
380
360
T /K
0
0.1
0.2
0.3
0.4
0.5
0.6
0.7
0.8
0.9
1
x_{H_2O}
b)
0.07
0.06
0.05
0.04
0.03
0.02
0.01
0
P /MPa
0
0.1
0.2
0.3
0.4
0.5
0.6
0.7
0.8
0.9
1
x_{H_2O}

Figure 7:

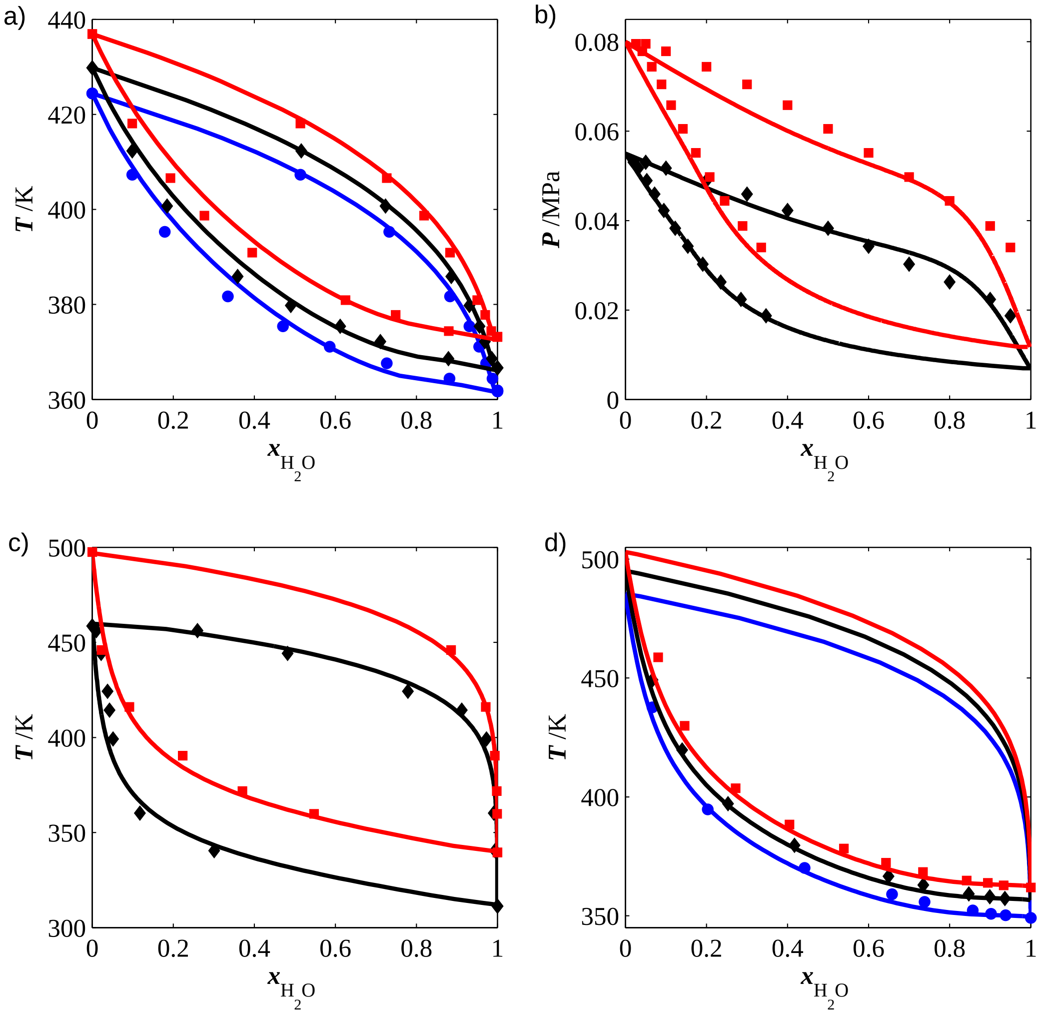
a)
440
420
400
380
360
T /K
0
0.2
0.4
0.6
0.8
1
x_{H_2O}
b)
0.08
0.06
0.04
0.02
0
P /MPa
0
0.2
0.4
0.6
0.8
1
x_{H_2O}
c)
500
450
400
350
300
T /K
0
0.2
0.4
0.6
0.8
1
x_{H_2O}
d)
500
450
400
350
T /K
0
0.2
0.4
0.6
0.8
1
x_{H_2O}

Figure 8:

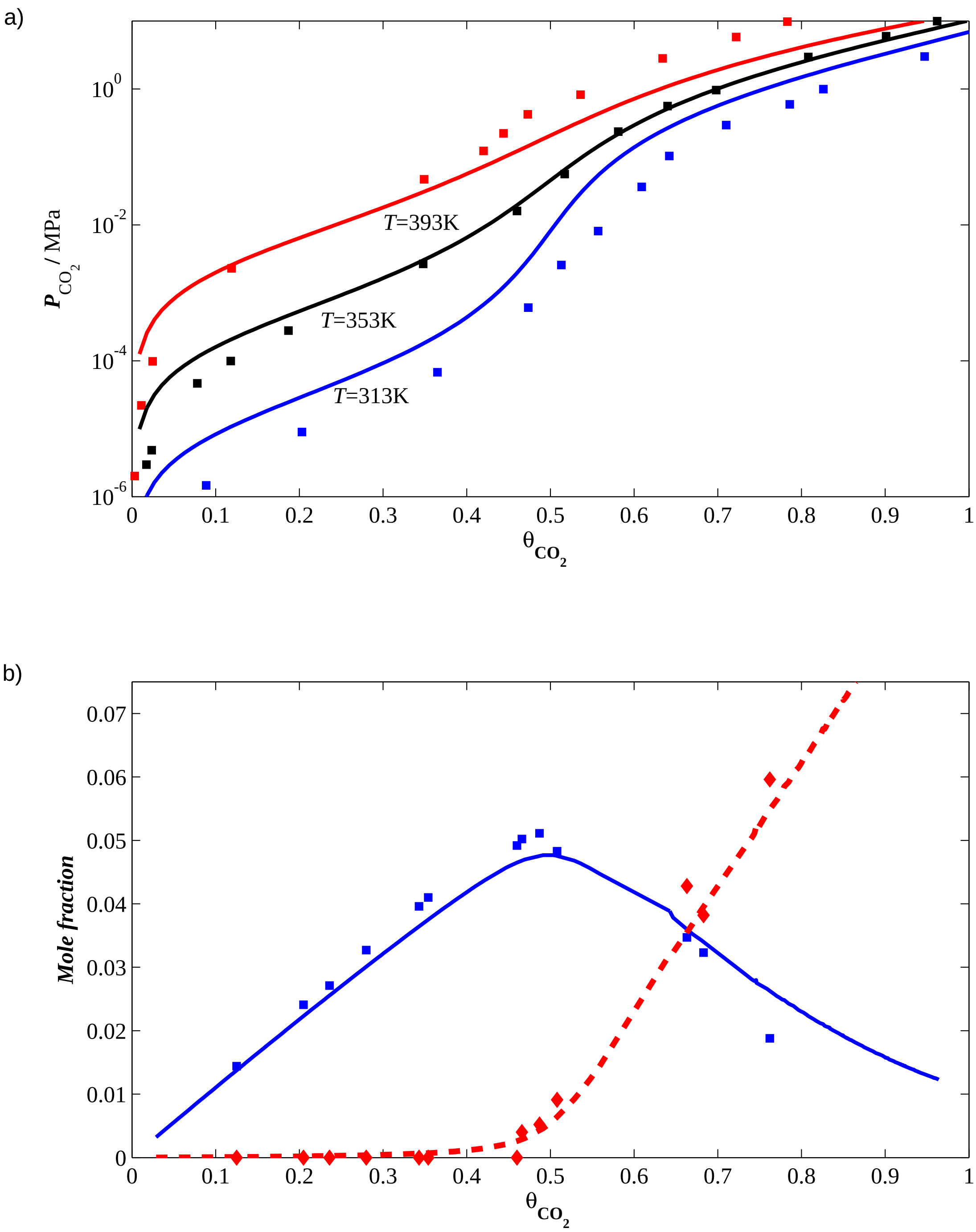
a)
P_{CO_2} / MPa
10^0
10^{-2}
10^{-4}
10^{-6}
T=393K
T=353K
T=313K
0
0.1
0.2
0.3
0.4
0.5
0.6
0.7
0.8
0.9
1
θ_{CO_2}
b)
Mole fraction
0.07
0.06
0.05
0.04
0.03
0.02
0.01
0
0
0.1
0.2
0.3
0.4
0.5
0.6
0.7
0.8
0.9
1
θ_{CO_2}

Figure 9:

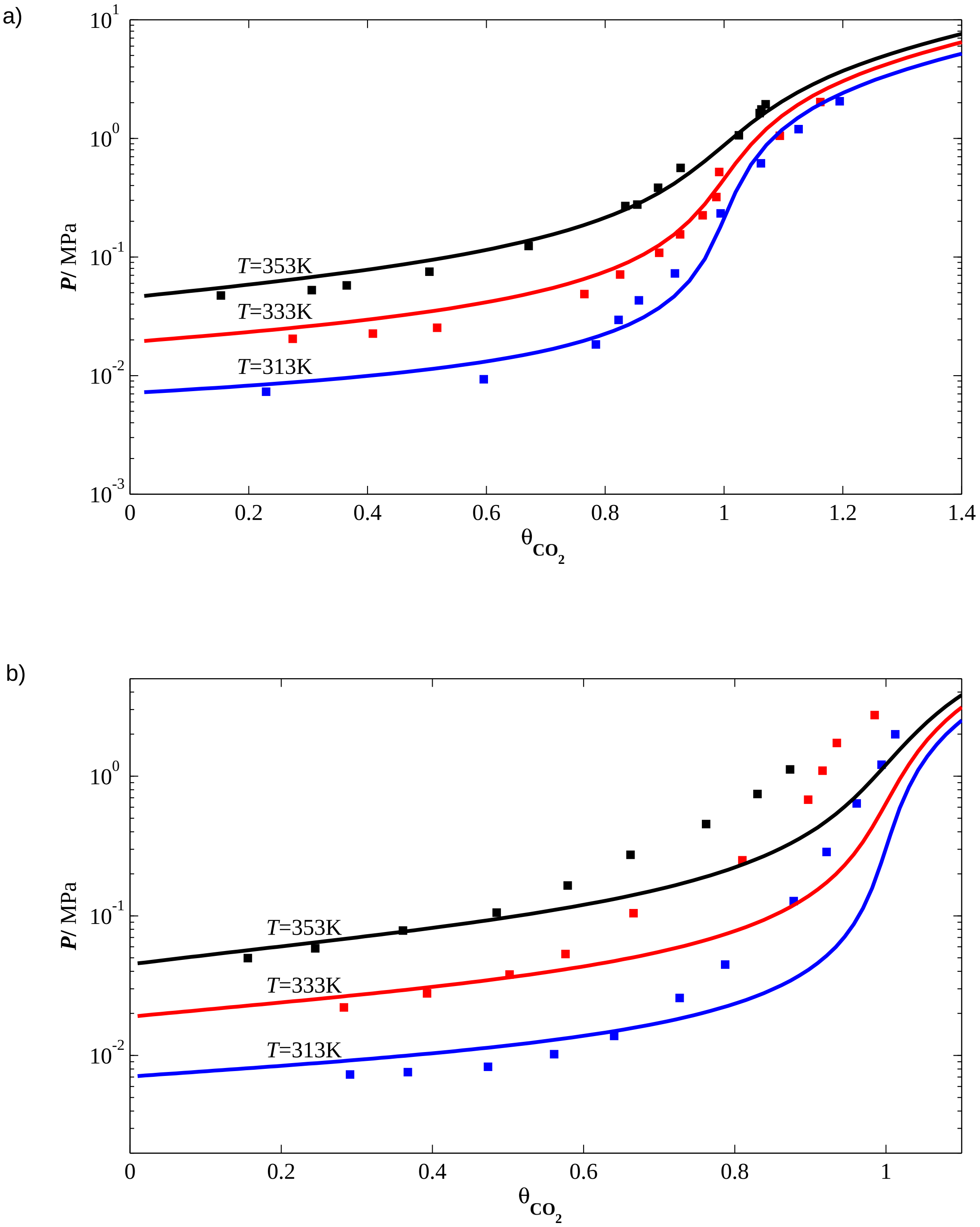
a)
10^1
10^0
10^{-1}
10^{-2}
10^{-3}
P/ MPa
T=353K
T=333K
T=313K
0
0.2
0.4
0.6
0.8
1
1.2
1.4
θ_{co_2}
b)
10^0
10^{-1}
10^{-2}
P/ MPa
T=353K
T=333K
T=313K
0
0.2
0.4
0.6
0.8
1
θ_{co_2}

Figure 10:

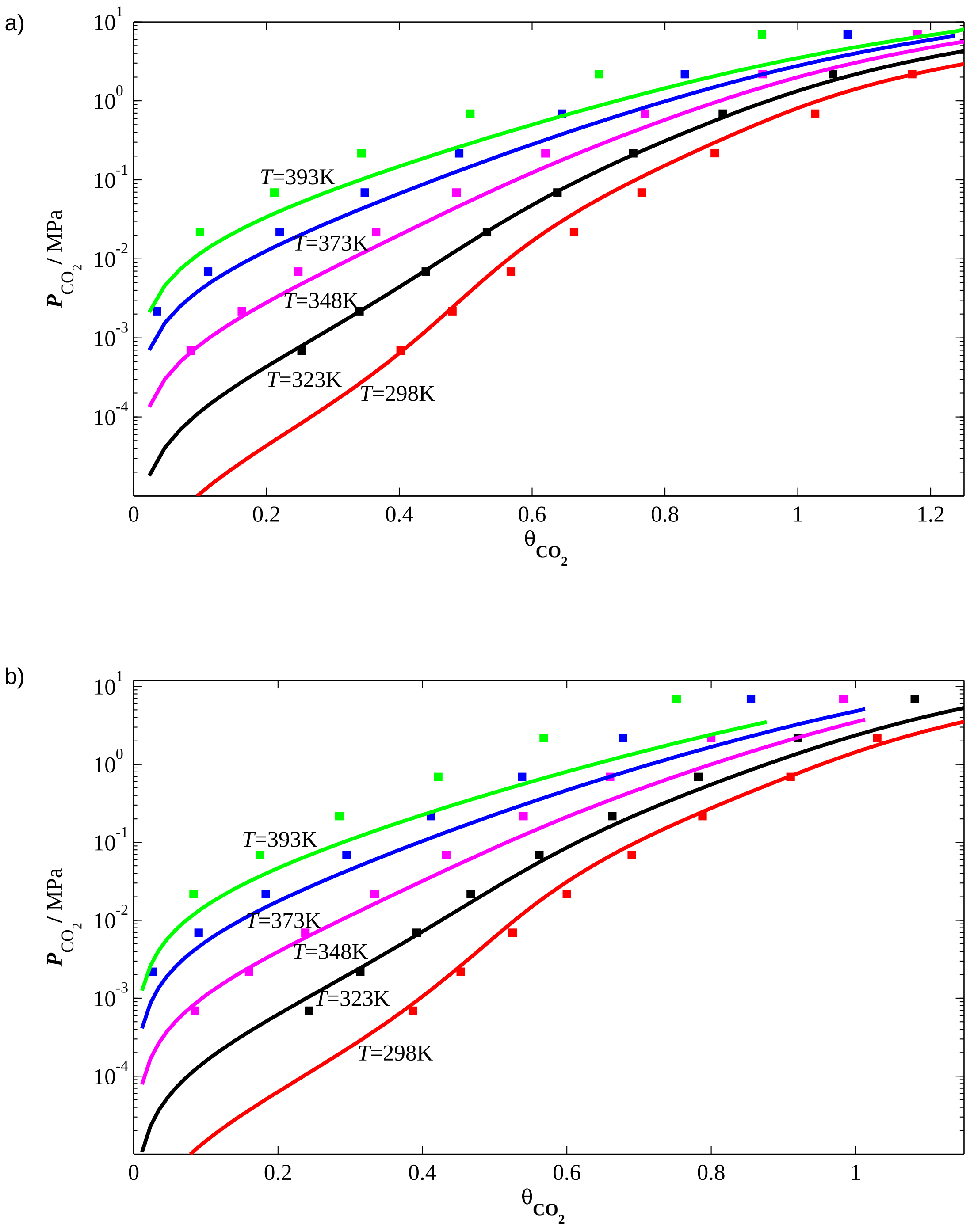
a)
10^1
10^0
10^{-1}
10^{-2}
10^{-3}
10^{-4}
P_{CO_2} / MPa
T=393K
T=373K
T=348K
T=323K
T=298K
0
0.2
0.4
0.6
0.8
1
1.2
θ_{CO_2}
b)
10^1
10^0
10^{-1}
10^{-2}
10^{-3}
10^{-4}
P_{CO_2} / MPa
T=393K
T=373K
T=348K
T=323K
T=298K
0
0.2
0.4
0.6
0.8
1
θ_{CO_2}

Figure 11:

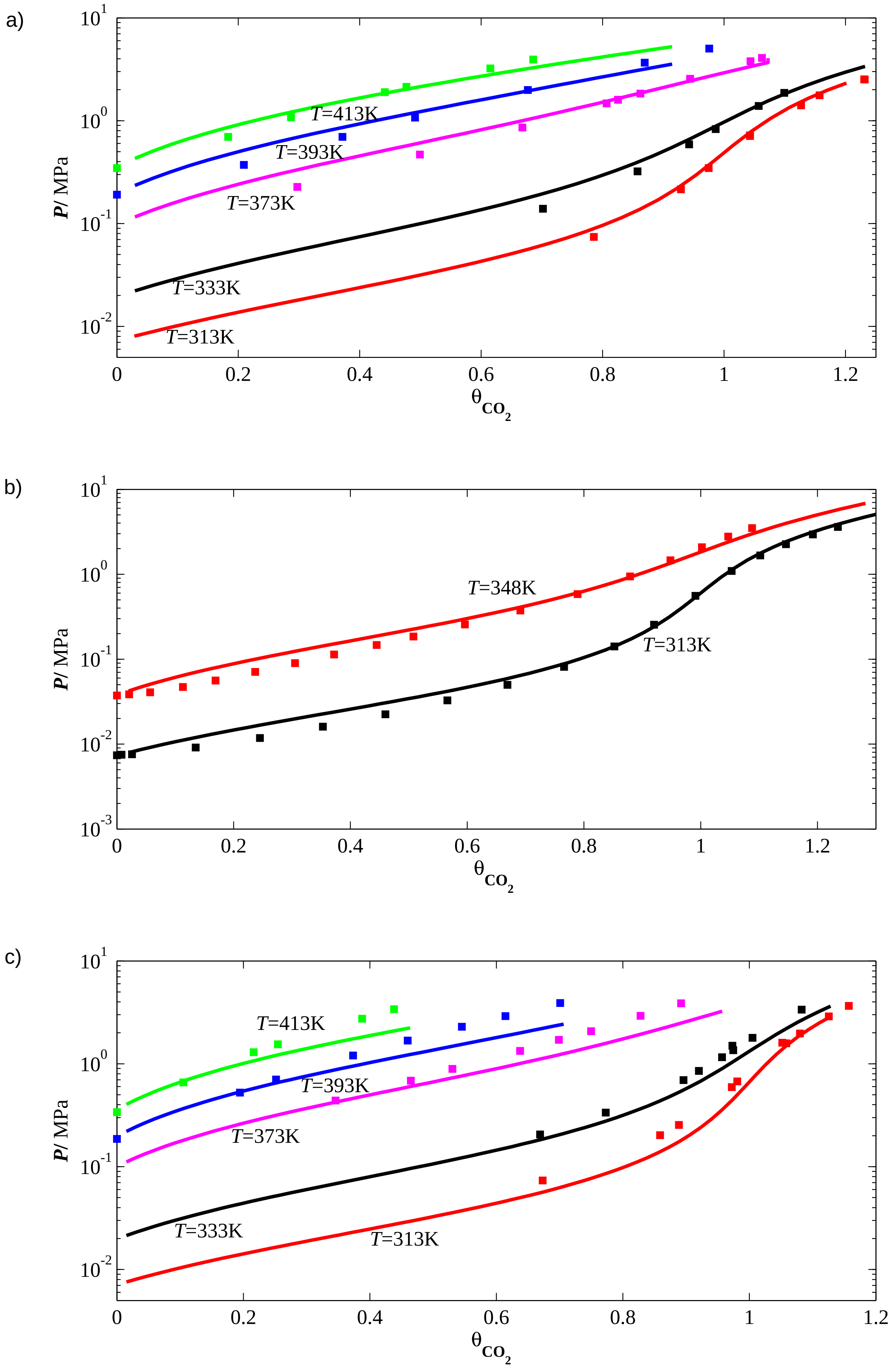
a)
10^1
10^0
10^{-1}
10^{-2}
P/ MPa
0
0.2
0.4
0.6
0.8
1
1.2
θ_{CO_2}
T=413K
T=393K
T=373K
T=333K
T=313K
b)
10^1
10^0
10^{-1}
10^{-2}
10^{-3}
P/ MPa
0
0.2
0.4
0.6
0.8
1
1.2
θ_{CO_2}
T=348K
T=313K
c)
10^1
10^0
10^{-1}
10^{-2}
P/ MPa
0
0.2
0.4
0.6
0.8
1
1.2
θ_{CO_2}
T=413K
T=393K
T=373K
T=333K
T=313K

Figure 12: